Cell Reports

Article

Excessive free fatty acid sensing in pituitary lactotrophs elicits steatotic liver disease by decreasing prolactin levels

Graphical abstract

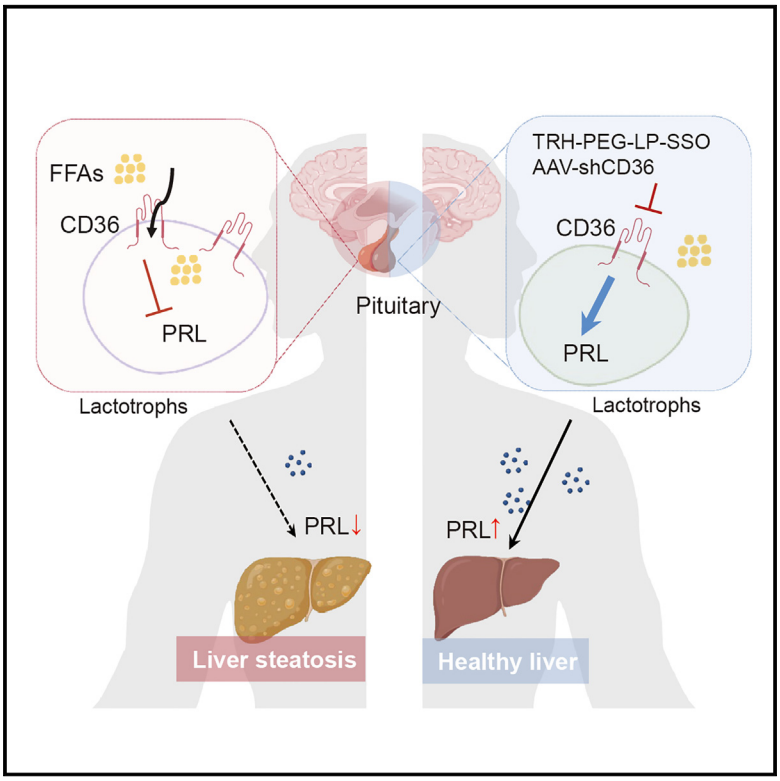

Highlights

- Elevated free fatty acids promote liver steatosis by suppressing prolactin levels
- FFAs inhibit PRL expression through excessive FFA sensing mediated by CD36 in lactotrophs
- Targeted CD36 inhibition in pituitary alleviates liver steatosis by elevating PRL levels

Authors

Xinlu Ji, Hongli Yin, Tianwei Gu, ..., Yuanyuan Nie, Pengzi Zhang, Yan Bi

Correspondence

zhang_pengzi@163.com (P.Z.), biyan@nju.edu.cn (Y.B.)

In brief

Ji et al. report that excessive FFA sensing in pituitary lactotrophs elicits hepatic steatosis by decreasing PRL levels via inhibition of the synthesis and secretion of PRL. Inhibiting excessive FFA uptake in the pituitary effectively elevates PRL levels and ameliorates liver steatosis.

Ji et al., 2024, Cell Reports *43*, 114465
July 23, 2024
https://doi.org/10.1016/j.celrep.2024.114465

CellPress

Cell Reports

CellPress
OPEN ACCESS

Article

Excessive free fatty acid sensing in pituitary lactotrophs elicits steatotic liver disease by decreasing prolactin levels

Xinlu Ji,[1,2,3] Hongli Yin,[1,2,3] Tianwei Gu,[1,2,3] Hao Xu,[1,2] Da Fang,[1,2] Kai Wang,[1,2] Haixiang Sun,[1,2] Sai Tian,[1,2] Tianyu Wu,[1,2] Yuanyuan Nie,[1,2] Pengzi Zhang,[1,2,*] and Yan Bi[1,2,4,*]

[1]Department of Endocrinology, Endocrine and Metabolic Disease Medical Center, Nanjing Drum Tower Hospital, Affiliated Hospital of Medical School, Nanjing University, Nanjing, China

[2]Branch of National Clinical Research Centre for Metabolic Diseases, Nanjing, China

[3]These authors contributed equally

[4]Lead contact

*Correspondence: zhang_pengzi@163.com (P.Z.), biyan@nju.edu.cn (Y.B.)

https://doi.org/10.1016/j.celrep.2024.114465

SUMMARY

The pituitary is the central endocrine gland with effects on metabolic dysfunction-associated steatotic liver disease (MASLD). However, it is not clear whether the pituitary responds to free fatty acid (FFA) toxicity, thus dysregulating hepatic lipid metabolism. Here, we demonstrate that decreased prolactin (PRL) levels are involved in the association between FFA and MASLD based on a liver biospecimen-based cohort. Moreover, overloaded FFAs decrease serum PRL levels, thus promoting liver steatosis in mice with both dynamic diet intervention and stereotactic pituitary FFA injection. Mechanistic studies show that excessive FFA sensing in pituitary lactotrophs inhibits the synthesis and secretion of PRL in a cell-autonomous manner. Notably, inhibiting excessive lipid uptake using pituitary stereotaxic virus injection or a specific drug delivery system effectively ameliorates hepatic lipid accumulation by improving PRL levels. Targeted inhibition of pituitary FFA sensing may be a potential therapeutic target for liver steatosis.

INTRODUCTION

Recently, the nomenclature of metabolic dysfunction-associated steatotic liver disease (MASLD) has been chosen to replace non-alcoholic fatty liver disease after four rounds of Delphi surveys.[1] MASLD is defined as the presence of hepatic steatosis with at least one of five cardiometabolic risk factors.[2] Over the recent decades, MASLD has emerged as the most common chronic liver disorder, with a prevalence of 32.4% worldwide,[3] and causes significant burdens to patients and society.[4,5] Currently, effective therapies for MASLD are limited.

The hallmark of MASLD is the accumulation of hepatic triglycerides (TGs), mainly driven by obesogenic environmental factors. The excessive levels of free fatty acids (FFAs) associated with overnutrition have deleterious effects on hepatic lipid metabolism. Clinical studies indicate that chronic elevation of serum FFA levels is closely associated with steatotic liver disease.[6] Higher plasma FFA levels are associated with a 0.38- to 2.60-fold increase in the risk of steatotic liver disease.[7,8] Mechanistic studies indicate that elevated FFA levels increase the uptake of hepatic fatty acids and *de novo* lipogenesis while impairing fatty acid oxidation and lipid export and driving the accumulation of TGs in the liver. Moreover, excess levels of circulating FFAs caused by accelerated lipolysis trigger proinflammatory processes in adipose tissue, leading to peripheral insulin resistance and ectopic fat accumulation.[9] FFA-derived toxic lipids drive inflammation and impair insulin signaling in skeletal muscle. This impedes insulin-stimulated glucose uptake in skeletal muscle and increases glucose delivery to the liver, further driving hepatic lipid synthesis.[10]

The central nervous system has critical roles in the maintenance of lipid homeostasis via neural and hormonal routes. Compared with rapid neural regulation, hormonal regulation is relatively stable and more sensitive to fatty acid toxicity, especially in chronic pathological conditions. The pituitary, the master endocrine gland of the central nervous system, releases adenohypophyseal hormones, which are required for growth and development. Notably, recent studies have emphasized the role of hormonal cross-talk between the pituitary gland and the liver in maintaining lipid homeostasis, as the thyroid-stimulating hormone increases hepatic TG content, whereas prolactin (PRL) and growth hormone (GH) improve liver steatosis.[11–14] However, it is not clear whether the pituitary gland responds to FFA toxicity, thus dysregulating hepatic lipid metabolism.

Here, we reported that excessive FFA sensing in pituitary lactotrophs elicited hepatic steatosis by decreasing PRL levels via inhibition of the synthesis and secretion of PRL in a cell-autonomous manner. Notably, inhibiting excessive lipid uptake using pituitary stereotaxic virus injection or a specific drug delivery system effectively ameliorated hepatic lipid accumulation by

improving PRL levels. These results advance our knowledge of mechanisms linking FFAs and MASLD, provide insights into the role of metabolite sensing in the pituitary gland, and highlight potential therapeutic targets for MASLD treatment.

RESULTS

Decreased PRL levels were involved in the association between FFAs and MASLD

A total of 328 subjects (64 controls and 264 with MASLD; mean age: 31.22 ± 8.12 years; mean BMI: 35.22 ± 3.78 kg/m^2) were recruited into the study based on liver biopsy results (Figure 1A). Compared with the controls, subjects with MASLD had higher levels of waist circumference, hemoglobin A1c (HbA1c), fasting blood glucose, fasting insulin, homeostatic model assessment of insulin resistance (HOMA-IR), alanine aminotransferase, aspartate aminotransferase, TG, and total cholesterol (all $p < 0.05$, Table 1). Serum FFA levels were significantly higher in the patients with MASLD than in the controls (Figure 1B). The individuals were further divided into four groups according to the quartiles of FFA levels (range from Q1 to Q4: <0.44, 0.44–0.52, 0.53–0.65, and >0.65 mmol/L, Table S1). We found that the serum FFA concentration was positively associated with the prevalence of MASLD as well as the degree of liver steatosis (p for trend < 0.001, Figure 1C). Moreover, after adjustment for age, sex, BMI, blood glucose levels, HOMA-IR, liver enzymes, and lipid profiles, logistic analysis revealed that higher FFA levels were associated with a higher risk of MASLD (odds ratio [OR]: 1.645, $p < 0.05$, Figure 1D). Similarly, subgroup analysis of individuals with normal glucose tolerance showed that patients with MASLD exhibited higher FFA levels compared with the controls (Table S2), and multivariate analyses showed that increasing FFAs was a risk factor for MASLD (OR: 1.973, $p < 0.05$, Table S3).

Next, to address the role of pituitary hormones in FFA-associated MASLD, serum levels of PRL, adrenocorticotropic hormone (ACTH), thyrotropin-stimulating hormone (TSH), luteinizing hormone (LH), follicle-stimulating hormone (FSH), and GH were analyzed across FFA quartiles. We observed a marked decrease in the levels of PRL and GH across FFA quartiles (Table S1; Figure 1E). Partial correlation analyses revealed a negative correlation between FFAs and PRL ($r = -0.174$, $p < 0.05$, Figure 1F) and GH ($r = -0.198$, $p < 0.05$) after adjustment of age, sex, BMI, HbA1c, HOMA-IR, and liver enzymes, whereas no correlation was observed between FFAs and TSH, ACTH, FSH, or LH. Moreover, PRL levels correlated negatively with the degree of liver steatosis ($r = -0.221$, $p < 0.05$), but no correlation was found between steatosis and TSH, ACTH, FSH, LH, or GH (Figure 1G). Logistic regression analyses indicated that decreased PRL levels, but not other pituitary hormones, were the only independent predictor of MASLD (OR: 0.853, $p < 0.05$, Table S4). Importantly, mediation analysis revealed that decreased PRL levels caused the correlation between FFAs and MASLD, with a mediation effect of 29.1% after adjustment for age, sex, BMI, HbA1c, HOMA-IR, and liver enzymes (95% confidence interval: 0.049–0.315, $p < 0.05$, Figure 1H). These data indicated that decreased PRL levels mediated the positive correlation between FFAs and MASLD.

Elevated FFAs induced liver steatosis by suppressing PRL levels

To further investigate the changes among the levels of FFAs, pituitary hormones, and the occurrence of liver steatosis, mice were dynamically fed with chow diet or high-fat diet (HFD; the results of body weight, glucose tolerance tests, and biochemical measurements for diet-induced mice are shown in Figures S1A–S1F). Profiles of hepatic lipid deposition, serum FFAs, and pituitary hormone levels were evaluated biweekly (Figure 2A). Importantly, when dynamically compared with chow-fed mice, HFD-fed mice exhibited higher serum FFA levels after 4 weeks (Figure 2B), lower serum PRL levels after 8 weeks (Figure 2C), and higher hepatic TG levels and liver steatosis after 10 weeks (Figures 2D and 2E) on the diets. In addition, the levels of other pituitary hormones, including GH, ACTH, FSH, LH, and TSH, did not differ significantly between chow-fed and HFD-fed mice (Figure S1G).

Furthermore, DMSO (vehicle) and C16-Bodipy (5 and 10 mM, respectively) were stereotactically injected into the pituitary of chow-fed mice to explore the effect of FFAs on pituitary PRL in the occurrence of liver steatosis (Figures 2F and 2G). Compared with the chow-fed mice, the HFD-fed mice showed higher levels of FFAs (Figure 2H) and lower levels of PRL in the pituitary (Figure 2I). Interestingly, the mice stereotactically injected with 10 mM C16-Bodipy exhibited significantly decreased circulating PRL levels compared with DMSO-treated mice after 24 h of injection (Figure 2J). Additionally, C16-Bodipy-treated mice exhibited higher levels of hepatic TG and hepatic lipid droplets than DMSO-treated mice (Figures 2K and 2L).

Moreover, FFA-treated HepG2 cells were cocultured with MMQ cells to evaluate the effect of PRL on hepatocytic steatosis *in vitro* (Figure 2M). TG quantification assays and oil red O staining revealed that increased PRL levels could markedly alleviate FFA-induced lipid accumulation in HepG2 cells in a dose-dependent manner (Figures 2N and 2O). Taken together, these results indicate that elevated levels of FFAs significantly suppressed the levels of circulating PRL, thus promoting liver steatosis.

Excessive FFAs inhibited the synthesis and secretion of PRL in a cell-autonomous manner

Serum FFA components include saturated and unsaturated fatty acids. To further identify the pathogenic fatty acids in the occurrence of steatotic liver disease, we identified the lipidomic profiles of serum FFAs in humans and diet-induced mice using gas chromatography-mass spectrometry (Figures 3A and 3B; Tables S5 and S6). When compared with those in controls, 8 fatty acids were up-regulated in individuals with biopsy-proven MASLD, and 15 fatty acids were up-regulated in HFD-fed mice (Figure 3C). Among the up-regulated fatty acids, palmitic acid (PA; C16:0), oleic acid (OA; C18:1n9), α-linolenic acid (α-LA; C18:3n3), and arachidic acid (AA; C20:0) were elevated in both humans and mice (Figure 3D). To determine whether these fatty acids dysregulated PRL levels, we treated MMQ cells with PA, OA, AA, α-LA, or their respective solvents. The PRL levels in cell culture supernatant were significantly reduced in PA-, OA-, and AA-treated lactotrophs when compared with the controls (Figure 3E) without affecting cell viability (Figure 3F).

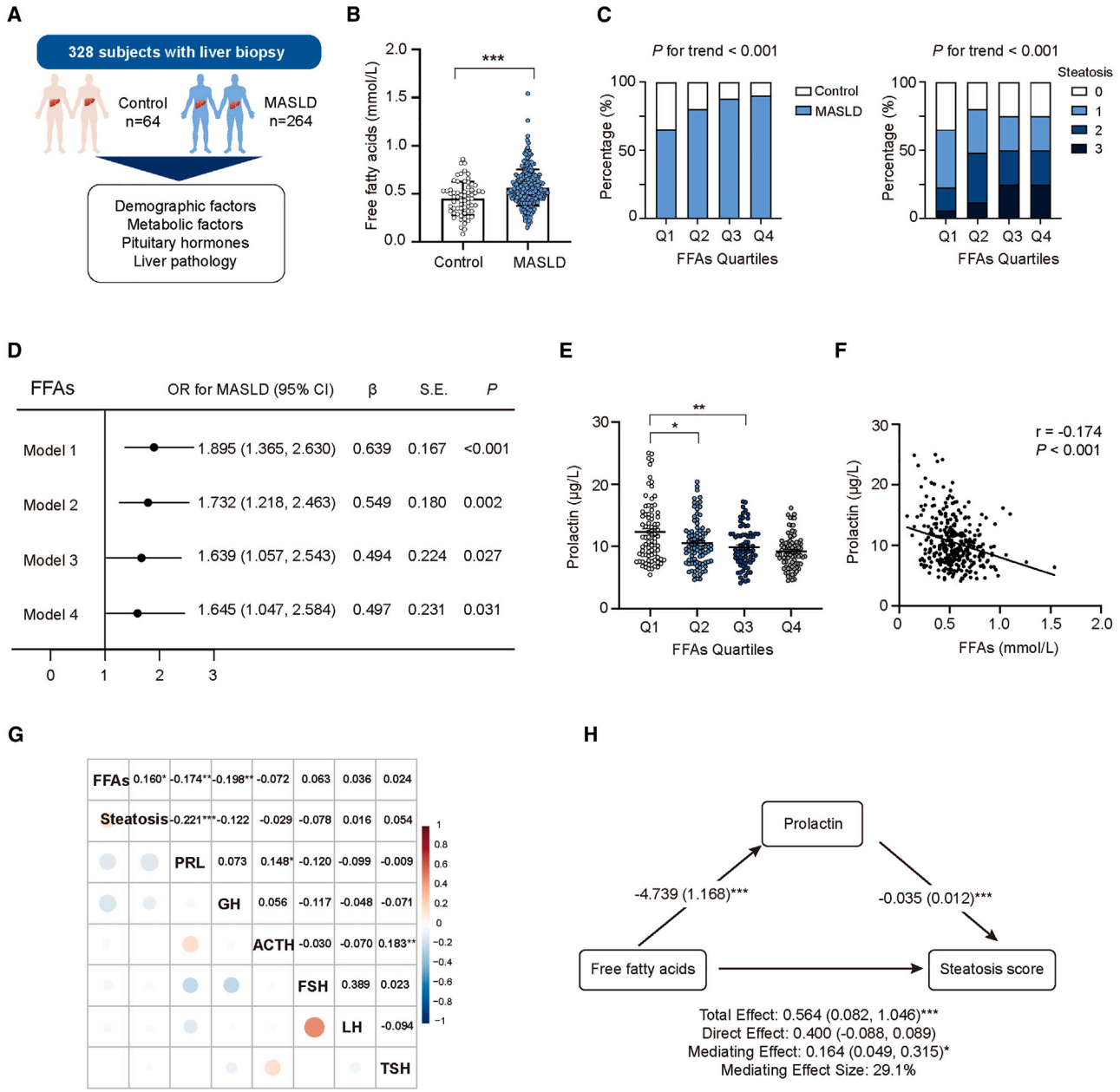

Figure 1. The association between FFAs and MASLD was mediated by decreased PRL levels

(A) Clinical scheme of 328 subjects with liver biopsy.

(B) Serum levels of free fatty acids (FFAs) in controls and patients with metabolic dysfunction-associated steatotic liver disease (MASLD).

(C) The percentage of MASLD across FFA quartiles (left) and associations between FFA quartiles and liver steatosis score (right). The quartile ranges of Q1, Q2, Q3, and Q4 of serum FFA levels were <0.44, 0.44–0.52, 0.53–0.65, and >0.65 mmol/L, respectively.

(D) Logistic regression analyses producing Odds ratio (OR) with 95% confidence intervals (95% CI) for MASLD. Model 1: unadjusted; model 2: adjusted for age, sex, BMI, blood pressure, and presence of diabetes; model 3: adjusted for model 2 and HbA1c, fasting blood glucose (FBG), HOMA-IR, alanine aminotransferase (ALT), and aspartate aminotransferase (AST); model 4: adjusted for model 3 and triglyceride (TG), total cholesterol (TC), high-density lipoprotein-cholesterol (HDL-c), and low-density lipoprotein-cholesterol (LDL-c).

(E) Serum levels of prolactin (PRL) across FFA quartiles in the cohort.

(F) Correlation analysis between FFA and PRL levels.

(G) Heatmap with a partial correlation coefficient between pituitary hormones and FFAs as well as steatosis severity after adjustment for sex, age, BMI, HbA1c, HOMA-IR, ALT, and AST.

(H) Associations of FFAs, the mediator of decreased levels of PRL, and steatosis score in the mediation model adjusted for sex, age, BMI, HbA1c, HOMA-IR, ALT, and AST.

*$p < 0.05$, **$p < 0.01$, and ***$p < 0.001$.

Table 1. Characteristics of the study individuals

Characteristics	Total population (*n* = 328)	Control (*n* = 64)	MASLD (*n* = 264)	Control vs. MASLD
Demographic factors				
Age (years)	31.22 ± 8.12	29.75 ± 8.93	31.58 ± 7.89	0.095
Female (*n*, %)	236, 72.0	51, 79.7	185, 70.1	0.125
BMI (kg/m^2)	35.22 ± 3.78	34.99 ± 5.01	35.28 ± 3.43	0.138
SBP (mmHg)	137.85 ± 18.20	133.86 ± 20.42	138.81 ± 17.54	0.023
DBP (mmHg)	88.49 ± 13.26	84.35 ± 13.80	89.47 ± 12.96	0.003
WC (cm)	112.04 ± 11.08	109.20 ± 13.45	112.65 ± 10.42	0.020
IGR (*n*, %)	119, 36.3	20, 31.3	99, 37.5	0.351
Diabetes (*n*, %)	57, 17.4	3, 4.7	54, 20.5	0.003
Metabolic factors				
HbA1c (%)	6.10 ± 1.45	5.52 ± 0.97	6.24 ± 1.51	<0.001
FBG (mmol/L)	5.82 ± 2.00	4.97 ± 1.25	6.03 ± 2.10	<0.001
FINS (μIU/mL)	21.75 (14.83, 31.20)	15.30 (9.90, 20.17)	23.90 (16.35, 33.49)	<0.001
HOMA-IR	5.22 (3.42, 8.63)	3.13 (2.18, 4.36)	5.77 (4.07, 9.58)	<0.001
ALT (U/L)	34.60 (21.43, 63.18)	20.45 (14.90, 30.18)	41.00 (26.63, 74.85)	<0.001
AST (U/L)	23.75 (16.65, 37.98)	16.50 (14.28, 22.95)	26.90 (18.43, 41.50)	<0.001
TG (mmol/L)	1.95 ± 1.76	1.41 ± 0.72	2.08 ± 1.91	<0.001
TC (mmol/L)	4.90 ± 0.94	4.84 ± 1.10	4.91 ± 0.90	0.174
HDL-c (mmol/L)	1.06 ± 0.24	1.17 ± 0.27	1.03 ± 0.23	<0.001
LDL-c (mmol/L)	3.00 ± 0.79	3.02 ± 0.98	2.99 ± 0.74	0.493
FFAs (mmol/L)	0.54 ± 0.19	0.46 ± 0.18	0.56 ± 0.19	<0.001
Pituitary hormones				
PRL (μg/L)	9.79 (7.71, 12.47)	11.47 (8.66, 16.61)	9.47 (7.52, 12.00)	<0.001
GH (μg/L)	0.08 (0.05, 0.23)	0.14 (0.06, 0.37)	0.07 (0.05, 0.19)	0.001
ACTH (pmol/L)	4.31 (2.89, 6.48)	4.35 (2.93, 6.19)	4.31 (2.87, 6.60)	0.988
FSH (mIU/mL)	5.54 (3.91, 7.37)	5.69 (3.13, 8.38)	5.54 (4.02, 7.05)	0.821
LH (mIU/mL)	4.63 (2.89, 6.92)	4.57 (2.82, 7.63)	4.69 (2.91, 6.8)	0.880
TSH (mIU/L)	2.13 (1.54, 2.81)	1.82 (1.26, 2.81)	2.15 (1.6, 2.81)	0.060
Liver histopathologic characteristics				
Steatosis	1 (1, 2)	0 (0, 0)	2 (1, 2)	<0.001
Ballooning	1 (1, 1)	1 (1, 1)	1 (1, 1)	0.343
Lobular inflammation	1 (0, 1)	0 (0, 1)	1 (1, 1)	<0.001
Fibrosis	0 (0, 1)	0 (0, 0)	0 (0, 1)	0.341

Data are expressed as mean ± standard deviation or median (interquartile range). Statistical significance was defined as $p < 0.05$. *p* values are based on independent-sample t test and Mann-Whitney U test for continuous data. BMI, body mass index; DBP, diastolic blood pressure; WC, waist circumference; IGR, impaired glucose regulation; FBG, fasting blood glucose; FINS, fasting insulin; FFAs, free fatty acids; HbA1c, hemoglobin A1c; HDL, high-density lipoprotein; HOMA-IR, the homeostatic model assessment of insulin resistance; ALT, alanine aminotransferase; AST, aspartate aminotransferase; LDL, low-density lipoprotein; MASLD, metabolic dysfunction-associated steatotic liver disease; SBP, systolic blood pressure; TC, total cholesterol; TG, triglyceride; PRL, prolactin; GH, growth hormone; TSH, thyrotropin-stimulating hormone; ACTH, adrenocorticotropic hormone; LH, luteinizing hormone; FSH, follicle-stimulating hormone.

Given that PA and OA were the main constituents of the circulating FFA pool, a mixture of PA and OA (PAOA) or BSA (control) was used in subsequent experiments. Consistently, PAOA (≤75 μM) caused a significant dose-dependent reduction in the levels of PRL in cell culture supernatant when compared with the BSA group and did not induce apoptosis or impair cell viability (Figures 4A–4D). What's more, PAOA markedly inhibited the mRNA and protein expressions of PRL (Figures 4E–4G), indicating that PAOA could directly suppress the synthesis of PRL in lactotrophs. It is well established that Pit-1 controls the lineage fate of lactotrophs and regulates the transcription of *Prl*-encoding hormone products.[15] We, therefore, investigated the expression of Pit-1 in PAOA-treated lactotrophs. Importantly, the mRNA and protein expressions of Pit-1 were significantly decreased in PAOA-treated lactotrophs compared with the controls (Figures 4H and 4I). Moreover, transcriptional activity of the rat *Prl* promoter regulated by Pit-1 was significantly decreased in PAOA-treated lactotrophs compared with the BSA group (Figure 4J). These results suggested that lipotoxicity inhibited the

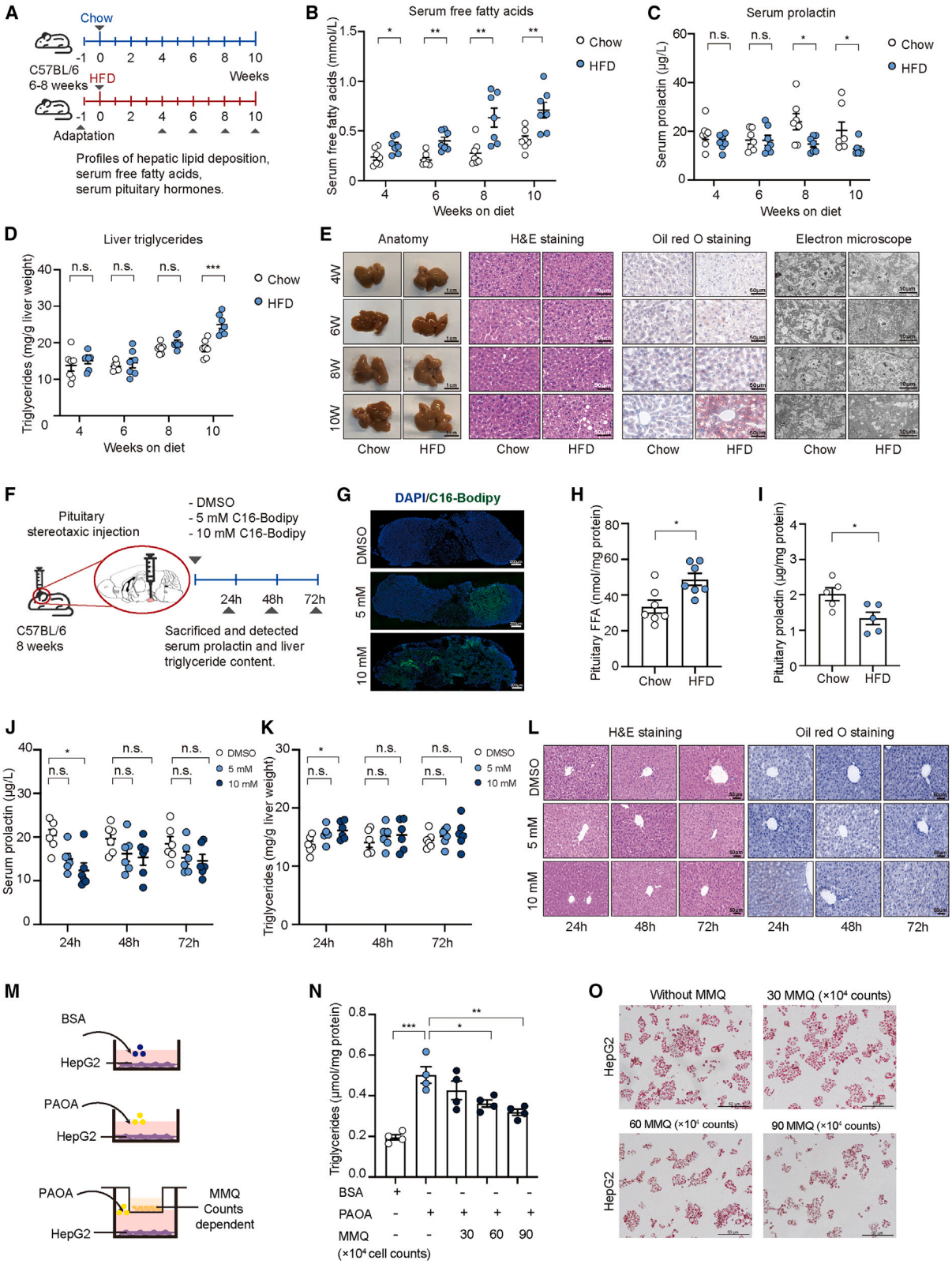

(legend on next page)

synthesis of PRL by decreasing the transcription activity of Pit-1 on the *Prl* promoter in lactotrophs.

In addition to synthesis, the mobilization of intracellular calcium ions and granule exocytosis plays an important role in the exocytosis process of PRL secretion.[16] Here, we found that intracellular calcium mobilization did not differ significantly between PAOA-treated lactotrophs and the control group (Figure 4K), whereas the gene expressions of *Snap25*, which is the factor involved in granule exocytosis of PRL, was significantly decreased in PAOA-treated lactotrophs when compared with the control group (Figure 4L). Moreover, dopamine (DA) that releases from tuberoinfundibular DA (TIDA) neurons in the hypothalamus serves as the major physiological inhibitor of PRL.[17,18] We thus investigated the effects of lipotoxicity on TIDA neurons in hypothalamus by measuring DA levels as well as dopaminergic neuronal activity. The results showed that there were no significant differences in the levels of hypothalamus DA between chow- and HFD-fed mice (Figure 4M), and immunofluorescent staining revealed that the HFD had no obvious effects on c-Fos colocalization with tyrosine hydroxylase-positive DA neurons in mice hypothalamus (Figure 4N).

Taken together, these data suggest that excessive FFAs directly inhibited the synthesis and secretion of PRL in a cell-autonomous manner rather than through activation of inhibitory neural circuits.

CD36-mediated excessive FFA sensing caused PRL inhibition in lactotrophs

Further, we assessed the PAOA-mediated lipid metabolism in MMQ cells *in vitro*. Bodipy 493/503 staining, oil red O staining, and TG quantification assays revealed more lipid accumulation in PAOA-treated lactotrophs than in the control group (Figure 5A). Flow cytometry-based fatty acid uptake assays revealed a significant increase in fatty acid uptake in PAOA-treated lactotrophs (Figure 5B). Thereafter, we detected the mRNA expressions of genes related to fatty acid uptake and found that only the gene expression of *Cd36*, but not *Gprs* or *Fatps*, was significantly elevated in PAOA-treated lactotrophs compared with the control group (Figure 5C). Additionally, the protein expression levels of CD36 were significantly up-regulated by lipotoxicity in both PAOA-treated lactotrophs and the pituitary of HFD-fed mice when compared with their respective controls (Figure 5D). Furthermore, inhibition of CD36 via sulfo-N-succinimidyl oleate (SSO) significantly reduced excessive fatty acid uptake and TG contents (Figures 5E and 5F) and increased the mRNA and protein expressions of PRL in PAOA-treated cells (Figures 5G and 5H). Besides, CD36 inhibition significantly up-regulated the mRNA expression of *Pit-1* in PAOA-treated lactotrophs (Figure 5I) and resulted in a marked increase in the transcriptional activity of *Prl* promoter activity in the presence of Pit-1 (Figure 5J). A lentivirus for CD36 knockdown (Lv-shCD36) or a negative control vector (Lv-NC) was transfected into the lactotrophs. The knockdown efficiency is shown in Figures 5K and 5L. Similarly, Lv-mediated CD36 knockdown decreased intracellular TG contents and increased PRL levels in PAOA-treated lactotrophs (Figures 5M and N). These results indicated that CD36 mediated excessive FFA sensing that inhibited PRL expression in lactotrophs.

Inhibition of CD36 in the pituitary alleviates liver steatosis by elevating PRL levels

To further evaluate whether inhibiting CD36 in the pituitary helps improve circulating PRL levels and alleviate liver steatosis *in vivo*, adeno-associated viruses (AAVs) expressing short hairpin RNA against CD36 (AAV-shCD36) or NC (AAV-NC) were stereotactically injected into the pituitary of diet-induced mice (Figure 6A). The knockdown efficiency is shown in Figures S2A and S2B. CD36 knockdown in mice pituitary had no effect on body weight and did not impair glucose tolerance or insulin sensitivity of mice fed a chow diet or HFD (Figures S2C–S2E). Noticeably, HFD-fed AAV-shCD36 mice exhibited higher circulating levels of PRL (Figure 6B) and significantly decreased liver weights and liver/body weight ratios compared with the HFD-fed AAV-NC mice (Figures 6C and 6D). Furthermore, the hepatic TG contents were significantly lower in HFD-fed AAV-shCD36 mice than those in the HFD-fed AAV-NC mice (Figure 6E). Histological analysis of liver sections revealed decreased severity of steatosis in HFD-fed AAV-shCD36 mice compared with those in the AAV-NC mice fed with the HFD (Figure 6F).

Next, we explored therapeutic potential of CD36 antagonist SSO targeting to the pituitary through a non-invasive approach. To this end, 8-week-old mice were intravenously injected with thyrotropin-releasing hormone (TRH)-polyethylene glycol-modified liposome (PEG-LP)-SSO (5 mg/kg), PEG-LP-SSO (5 mg/kg), or its control (PEG-LP-saline) once a week. The mice were then maintained on the chow diet or HFD diet for 10 weeks (Figure 6G). The schematic illustration, particle size, morphology, and entrapment efficiency of the TRH-PEG-LP delivery system are shown in Figures S3A–S3D. The fluorescent intensity in the pituitary of the TRH-PEG-LP-SSO mice was markedly higher than that in the PEG-LP-SSO group (Figure 6H). Consistently,

Figure 2. Elevated FFAs induced liver steatosis by suppressing PRL levels

(A) Experimental scheme of temporal diet-induced mice (n = 7 per group).

(B–E) Dynamic assays of serum levels of FFAs (B), serum PRL (C), liver TGs (D), and liver anatomy (scale bars, 1 cm), H&E staining (scale bars, 50 μm), oil red O staining (scale bars, 50 μm), and electron microscopy assays (scale bars, 10 μm) (E) in temporal diet-induced mice.

(F) Experimental scheme of pituitary stereotaxic C16-Bodipy-injected mice (n = 6 per group). C16-Bodipy, a fluorescently labeled palmitic acid.

(G) Fluorescence assays of C16-Bodipy in mice pituitary. Scale bars, 200 μm.

(H and I) Pituitary FFA content assays (H) and pituitary PRL content assays (I) in 10-week chow- and HFD-fed mice (n = 5–7 per group).

(J–L) Assays of serum levels of PRL (J), liver TGs (K), and H&E and oil red O staining assays (L) in mice injected with C16-Bodipy in pituitary. Scale bars, 50 μm.

(M) Experimental scheme of coculture system of MMQ cells and PAOA-induced HepG2 cells. n = 4 for independent experiments.

(N and O) Intracellular TG content assays (N) and oil red O staining assays (O) in HepG2 cells cocultured with or without MMQ cells. HepG2 cells were treated with 250 μM PAOA for 24 h. Scale bars, 50 μm.

The data are presented as mean ± SEM. *p < 0.05, **p < 0.01, and ***p < 0.001, n.s., not significant difference, vs. HFD-fed mice or DMSO-treated mice. Student's t test and one-way ANOVA were used for statistical analysis.

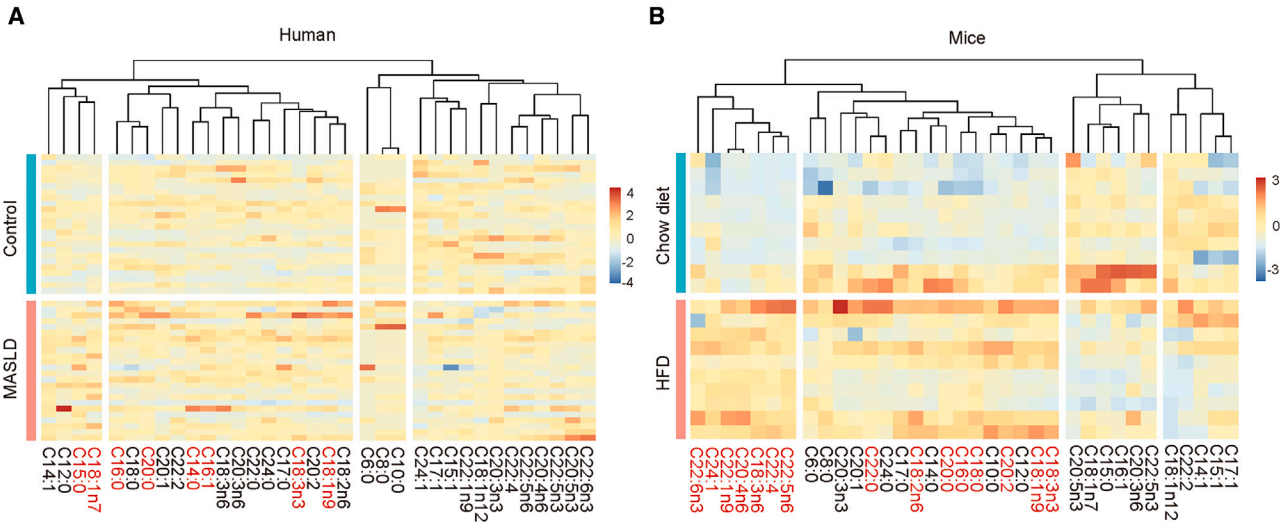

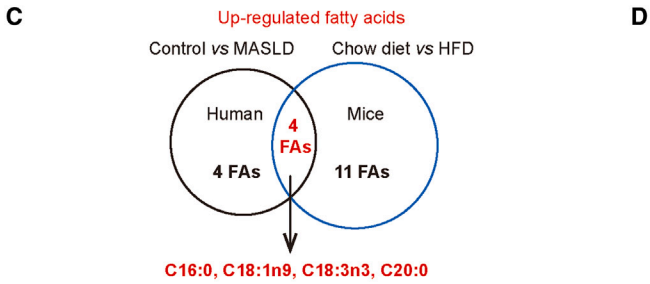

D

Fatty acids (μg/mL)	Human		Mice	
	Control	MASLD	Chow diet	HFD
C16:0	612.8 ± 58.6	661.4 ± 95.5	921.3 ± 134.6	1038.6 ± 89.4
C18:1n9	201.7 ± 37.3	247.2 ± 80.7	219.0 ± 70.8	303.5 ± 97.6
C18:3n3	11.1 ± 4.6	17.3 ± 7.6	5.3 ± 1.8	8.4 ± 3.2
C20:0	3.1 ± 0.4	3.5 ± 0.6	6.3 ± 1.3	7.2 ± 0.8

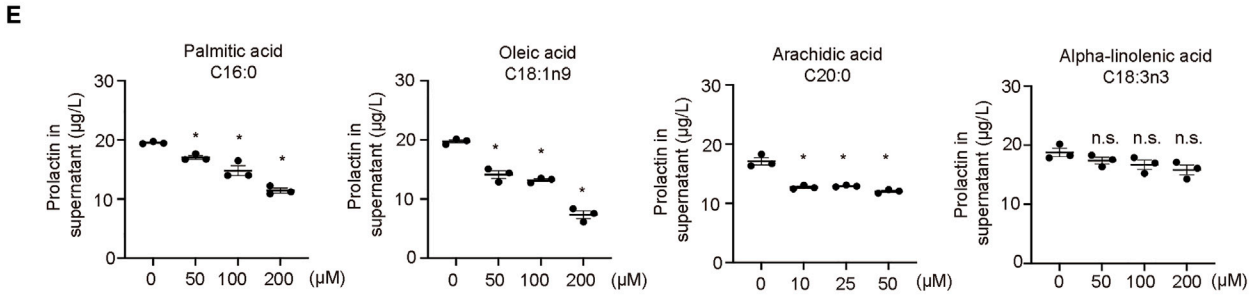

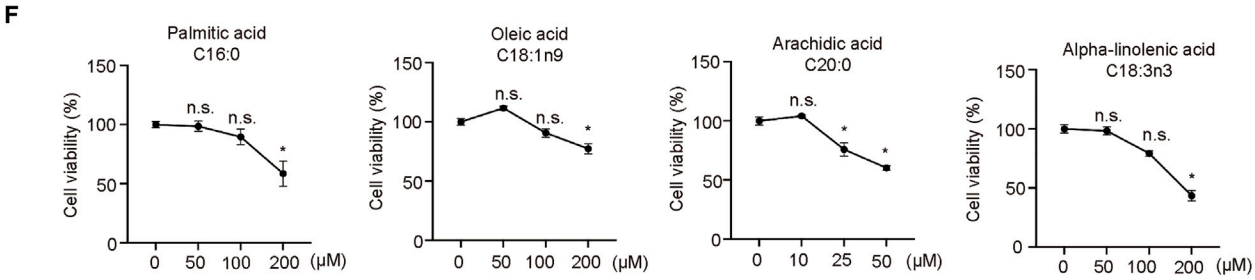

Figure 3. Identification of pathogenic FFAs in steatotic liver disease that suppressed PRL levels

(A) Gas chromatography-mass spectrometry (GCMS) analysis of serum fatty acids from patients with ($n = 24$) or without ($n = 24$) MASLD diagnosed by liver biopsy.

(B) GCMS analysis of serum fatty acids in 10-week chow- and HFD-fed mice ($n = 10$ per group).

(C) Screening map of up-regulated fatty acids in both patients with MASLD and HFD-fed mice.

(D) Quantifications of up-regulated fatty acids.

(E) Supernatant PRL content assays in MMQ cells treated with palmitic, oleic, arachidic, and alpha-linolenic acids.

(F) Cell viability assays.

The data are presented as mean ± SEM. *$p < 0.05$, n.s., not significant difference, vs. control vehicle group ($n = 3$ for independent experiments). One-way ANOVA was used for statistical analysis.

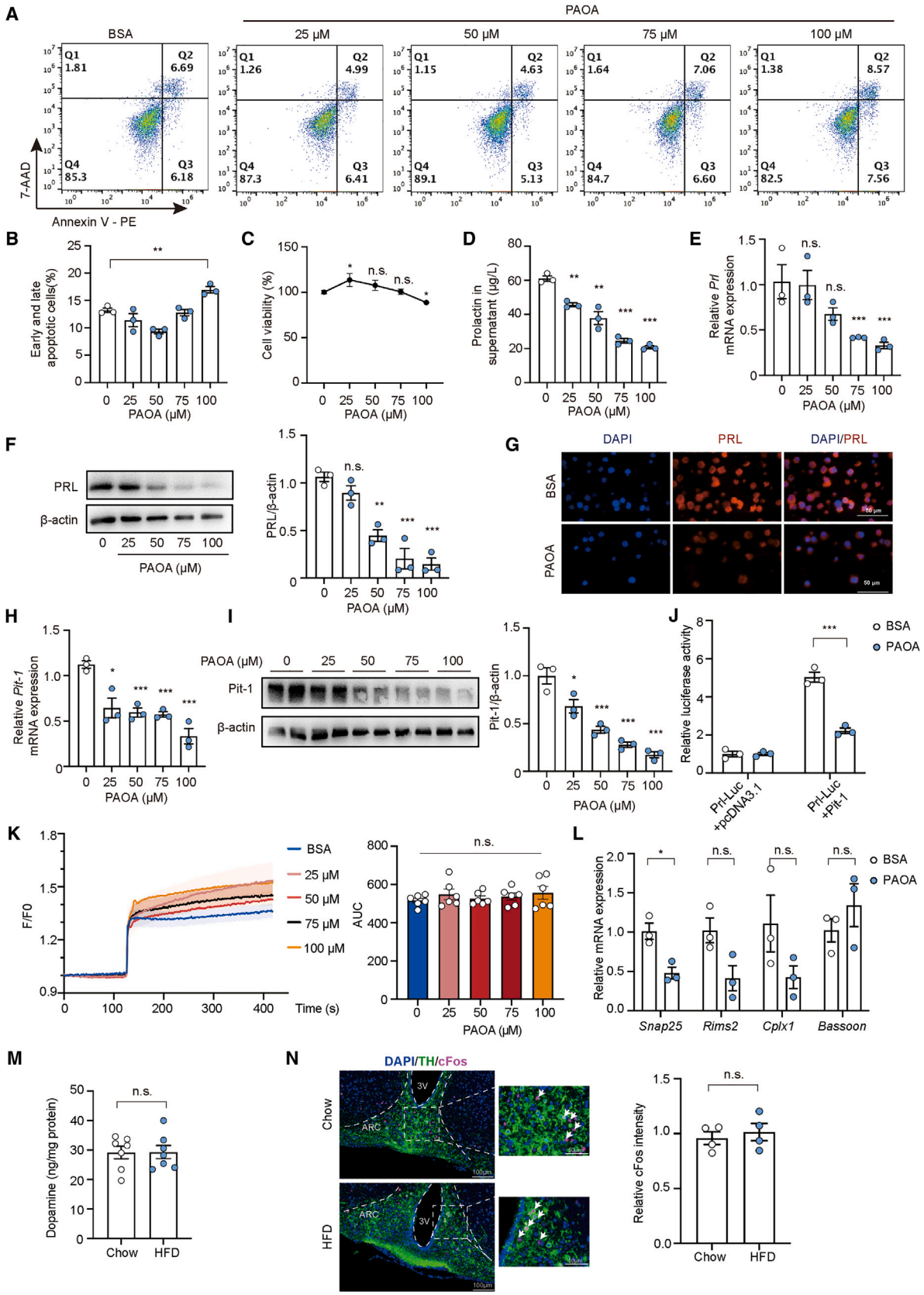

(legend on next page)

TRH-PEG-LP-SSO HFD-fed mice showed higher circulating PRL levels, fewer hepatic TG contents, and ameliorated liver steatosis compared with the control HFD-fed group and the PEG-LP-SSO HFD-fed group (Figures 6I–6K). Collectively, these results indicated that inhibition of CD36 targeted to mice pituitary could alleviate liver steatosis by improving PRL levels.

DISCUSSION

In the present study, we uncovered a mechanism of MASLD, in which pituitary lactotrophs sensed excessive FFA signals and decreased PRL levels, thereby eliciting hepatic steatosis. What's more, inhibiting excessive FFA uptake in the pituitary through stereotactic injection or a specific drug delivery system effectively increased circulating PRL levels and ameliorated hepatic steatosis (Figure 6L).

Chronic elevation of serum FFA levels contributes to steatotic liver disease.[6] Elevated circulating FFA levels, especially saturated long-chain fatty acids, increased MASLD risk by 0.38- to 2.06-fold.[7,8] Moreover, elevated FFAs associated with overnutrition are observed in subjects with obesity and type 2 diabetes.[19] Once elevated, FFAs will inhibit insulin's antilipolytic action, which further increases FFA release into the circulation.[20] Here, our findings are consistent with previous studies showing that serum FFAs, especially PA and OA, are elevated in individuals with biopsy-confirmed steatotic liver disease. Based on liver pathology, we found that elevated FFA levels are associated with a 64.5% rise in the risk of MASLD. To date, the mechanisms by which FFAs contribute to steatotic liver disease mainly focus on insulin resistance and chronic inflammation in peripheral tissues, particularly in adipose tissue.[21] Adipose dysfunction further contributes to overloaded FFAs from lipolysis and disturbs adipokines release, aggravating insulin resistance and promoting liver steatosis.[9,10] In addition, new evidence exists for the important relationships between MASLD and endocrine dysfunction beyond insulin resistance, including pituitary hormones, sex hormones, and steroid hormones, over the past decade.[14,22]

The pituitary as the central nervous system is the master endocrine gland and has been shown to influence the regulation of lipid and glucose metabolism. For example, higher TSH levels are correlated with worsening MASLD and stimulate hepatic lipogenesis,[11,23] while GH ameliorates liver steatosis by enhancing fatty acid oxidation.[24] PRL, beyond its traditional function in lactation and reproduction, has recently been reported to serve as a metabolic hormone to maintain and promote metabolic homeostasis. Numerous large cohort clinical studies have recently shown that lower circulating PRL levels are associated with higher risk of metabolic disease, including type 2 diabetes, MASLD, and obesity.[13,25–28] Recent studies, including ours, have found that PRL improves hepatic steatosis by suppressing the uptake of fatty acids and *de novo* lipogenesis,[13,29] supporting the multifaceted roles of PRL in the regulation of metabolism.

The pituitary gland locates outside the blood-brain barrier and is freely accessible to circulating fatty acids; nonetheless, few studies have assessed whether the pituitary responds to circulating fatty acids levels. In the present study, we reported that the pituitary gland, especially pituitary lactotrophs, sensed circulating FFA signals and participated in the regulation of hepatic lipid metabolism. Correlation analysis among levels of FFAs and pituitary hormones showed that FFA levels were negatively associated with PRL and GH but not TSH, ACTH, FSH, or LH levels. Logistic regression analyses showed that decreased PRL levels, but not those of other pituitary hormones, were a risk factor for MASLD independent of sex, age, BMI, HbA1c, HOMA-IR, and lipid levels. In addition, our analysis of dynamic HFD-induced mice and pituitary FFA-injected mice indicated that elevation of FFAs suppressed the levels of circulating PRL, thus promoting hepatic TG accumulation. Serum levels of other pituitary hormones, including GH, TSH, ACTH, FSH, and LH, did not differ significantly between 10-week diet-induced mice, possibly due to the short duration of diets intervention or negative feedback regulation. As a hormone that lacks a target endocrine gland, PRL is more likely to respond to exteroceptive stimuli, such as light and stress. Nevertheless, little research has focused on the role of PRL in response to fasting, cold, or adrenergic stimulation that affected adipose lipolysis on liver homeostasis by regulating circulating fatty acids.[30,31] There needs to be more research in the future to elucidate the role of PRL in response to environmental changes that regulate lipid metabolism. *In vivo*, PRL is synthesized in and secreted from the lactotrophs of the anterior pituitary gland.[32] Our mechanic studies revealed that FFA exposure significantly inhibited the mRNA and protein expressions of PRL in lactotrophs. Moreover, FFA exposure significantly decreased the gene expression of *Snap25*, the factor involved in granule exocytosis of PRL, whereas the intracellular calcium mobilization was not affected.

Figure 4. Excessive FFAs inhibited the synthesis and secretion of PRL in a cell-autonomous manner

(A–E) Cell apoptosis assays (A and B) and cell viability assays (C) in MMQ cells treated with PAOA (1:1). Supernatant PRL content assays (D), real-time PCR of *Prl* (E), and western blot analysis of PRL expression (F) in MMQ cells treated with BSA or PAOA (1:1) for 24 h.

(G) Immunofluorescence of PRL in MMQ cells treated with BSA or 75 μM PAOA. Scale bars, 50 μm.

(H and I) Real-time PCR of *Pit-1* (H) and western blot analysis of Pit-1 expression (I) in MMQ cells treated with BSA or PAOA (1:1) for 24 h.

(J) PRL luciferase activity of MMQ cells treated with BSA or 75 μM PAOA, with the levels in the blank group arbitrarily set to 1. The *Prl* promoter region was cloned into a pGL3-basic vector. Luciferase activity was determined by dual-luciferase reporter assays and normalized with internal control.

(K) Representative traces showing the effects of BSA and PAOA (25–100 μM) on intracellular calcium mobilization in MMQ cells.

(L) Real-time PCR analysis of gene expression associated with granule exocytosis of PRL in MMQ cells.

(M) Quantification of dopamine (DA) levels in hypothalamus of mice fed for 8 weeks with chow or HFD ($n = 7$ per group).

(N) Representative confocal images depicting tyrosine hydroxylase (TH) and c-Fos in dorsomedial hypothalamic arcuate nucleus of mice fed for 8 week with chow or HFD ($n = 4$ per group). TH is the rate-limiting enzyme for DA synthesis, and c-Fos is a reliable marker for neural activity. Scale bars, 100 μm (left) and 50 μm (right).

Data are presented as mean ± SEM. $^{*}p < 0.05$, $^{**}p < 0.01$, and $^{***}p < 0.001$, n.s., not significant difference, vs. BSA group ($n = 3$ for independent experiments). One-way ANOVA was used for statistical analysis.

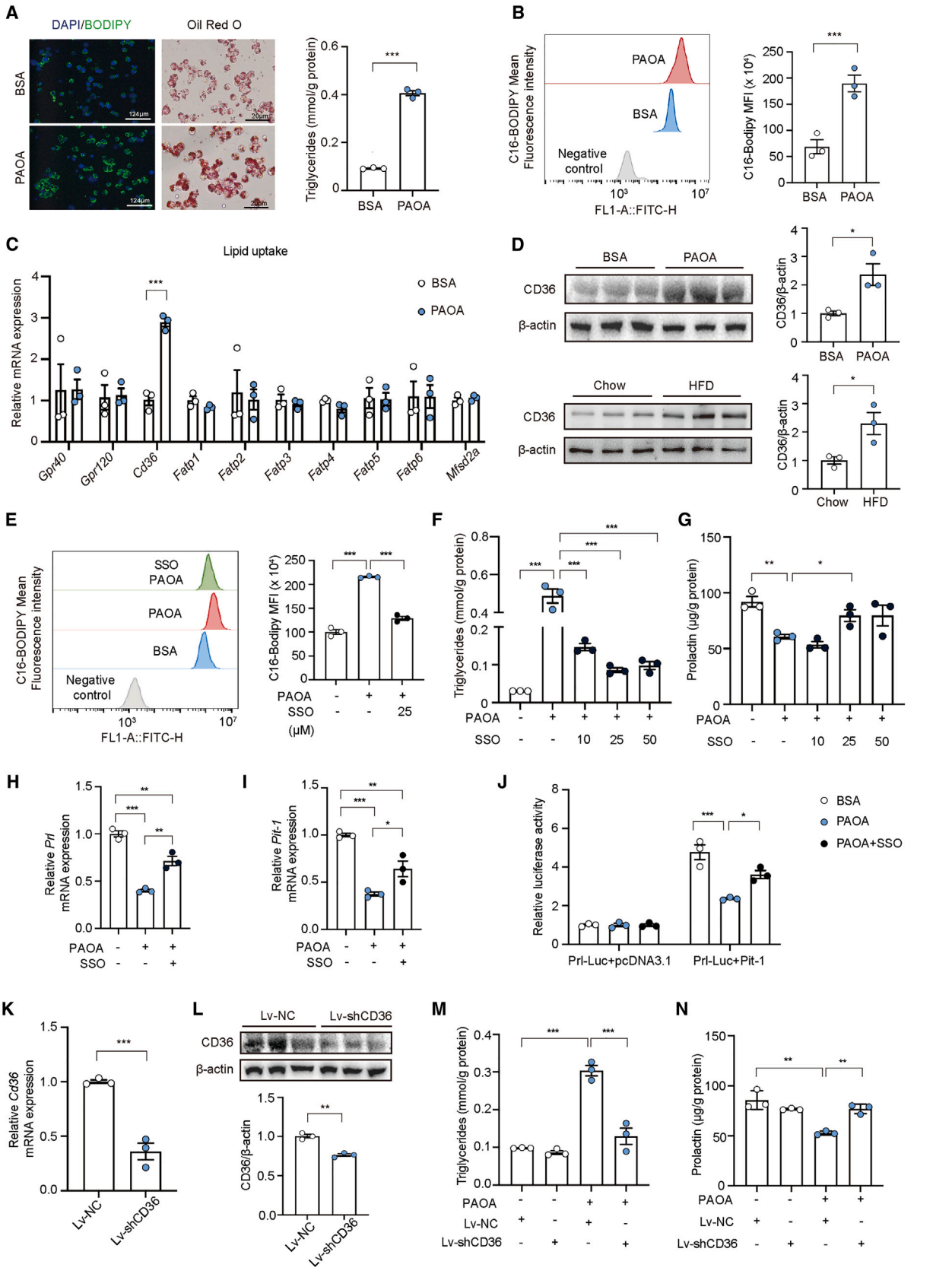

(legend on next page)

Besides the cell-autonomous response to FFA signals in lactotrophs, extracellular regulation mediated by dopaminergic neurons was also assessed. It is well reported that DA released from TIDA neurons in hypothalamus is the predominant inhibitor of PRL in the pituitary.[17] A previous study found that mice exposed to a chronic HFD for 5 months exhibited markedly increased DA levels.[33] In our study, the short duration of 8 weeks HFD had no effect on hypothalamus DA levels or DA neuronal activity. These results suggest that FFA toxicity directly inhibited the expression of PRL in an early cell-autonomous manner rather than through activation of inhibitory neural circuits.

CD36 is widely expressed in various cell types, including endothelial cells, hepatocytes, myocytes, and adipocytes. Increased CD36 levels in peripheral tissues facilitate FFA uptake and contributes to serious metabolic disorders, such as MASLD, diabetic cardiomyopathy, and atherosclerosis.[34–37] In this study, we demonstrated that CD36 in the pituitary, especially in lactotrophs, mediated excessive FFA sensing and promoted ectopic lipid deposition in lactotrophs. Importantly, pituitary CD36 silencing via stereotactic AAV-shCD36 injection significantly enhanced PRL levels and alleviated liver steatosis in HFD-fed mice. Nevertheless, the operation of stereotactic pituitary injection is complicated and may damage brain nerves and blood vessels. Therefore, how to increase the accumulation of drugs in the pituitary safely and effectively through a non-invasive basis is the key to treat pituitary and related diseases. Targeting ligands that bind specifically to the receptors on the targeted cells is a promising strategy that mediates targeted delivery.[38] In our study, SSO, a selective inhibitor of CD36,[39] was loaded into a TRH-guided LP (TRH-PEG-LP-SSO) to reduce the side effects and frequency of systemic administration. TRH is a tripeptide with high affinity to its receptor expressed in the pituitary, aiming to improve pituitary targetability.[40] Indeed, we found that TRH-PEG-LP-SSO can better specifically target pituitary *in vivo* than PEG-LP-SSO. Moreover, TRH-PEG-LP-SSO treatment can significantly elevate PRL levels and alleviate liver steatosis. Targeted delivery of SSO to antagonize CD36 in the pituitary by TRH-PEG-LP may be a promising treatment to manage MASLD and improve the serum levels of PRL. It also provides a potential delivery strategy for targeted therapy of other pituitary diseases.

In this study, we reported the role of fatty acid sensing mediated by CD36 in the pituitary, providing insights into metabolic regulation of the pituitary. Next, we identified a mechanism of MASLD in which the pituitary lactotrophs sensed excessive FFA signals and inhibited the synthesis and secretion of PRL, thus decreasing PRL levels and eliciting hepatic steatosis, broadening a cell-autonomous mechanism in PRL regulation affected by FFA toxicity. Moreover, we explored the drug delivery system of TRH-PEG-LP-SSO, which showed a better targeting property to the pituitary. Blocking of CD36-dependent FFA sensing in the pituitary significantly elevated PRL levels and alleviated liver steatosis, providing a potential therapeutic target in MASLD treatment.

Collectively, we presented evidence that the pituitary lactotrophs sensed excessive FFA signals and decreased PRL levels, thus eliciting hepatic steatosis. Inhibiting excessive lipid uptake in the pituitary can effectively elevate PRL levels and ameliorate HFD-induced steatotic liver disease.

Limitations of the study

This study has some limitations. First, pregnant females were excluded in our clinical cohort due to concerns about the great impact of pregnancy on PRL levels. Since PRL is a central hormone closely related to pregnancy, there needs to be more research to elucidate the cellular response to lipid signals in pituitary lactotrophs during pregnancy. Second, our pharmacological intervention to elevate PRL levels was unable to target specific types of pituitary cells (i.e., lactotrophs). Further research about a more precise delivery system selectively targeted to pituitary lactotrophs is needed to determine the therapeutic potential of elevating PRL levels in the treatment of MASLD.

STAR★METHODS

Detailed methods are provided in the online version of this paper and include the following:

- KEY RESOURCES TABLE
- RESOURCE AVAILABILITY
  - Lead contact
  - Materials availability
  - Data and code availability
- EXPERIMENTAL MODEL AND STUDY PARTICIPANT DETAILS
  - Human subjects
  - Animal models
  - Cell experiments
- METHOD DETAILS

Figure 5. CD36-mediated FFA sensing inhibited the expression of PRL in MMQ cells under FFA load

(A) Fatty acid accumulation, oil red O staining, and intracellular TG content assays in MMQ cells treated with BSA or 75 μM PAOA. Scale bars, 124 μm (left) and 20 μm (right).

(B) Flow cytometry-based fatty acid uptake assays in MMQ cells treated with BSA or 75 μM PAOA.

(C) Real-time PCR of genes related to lipid uptake pathway in MMQ cells treated with BSA or 75 μM PAOA.

(D) Western blot analysis of CD36 expression in 75 μM PAOA-treated MMQ cells and pituitary of 10-week HFD-fed mice, respectively.

(E) Flow cytometry-based fatty acid uptake assays in PAOA-induced MMQ cells pre-treated with 25 μM SSO or equal volume of DMSO.

(F and G) Cellular TG content assays (F) and supernatant PRL content assays (G) in MMQ cells treated with BSA or 75 μM PAOA.

(H and I) Real-time PCR analysis of mRNA levels of *Prl* (H) and *Pit-1* (I) in MMQ cells treated with BSA and PAOA (75 μM) with or without SSO (25 μM).

(J) PRL luciferase activity of the groups indicated, with the levels in the blank group arbitrarily set to 1.

(K) Real-time PCR analysis of *Cd36* expression.

(L) Western blot analysis of CD36 expression.

(M and N) Cellular TG content assays (M) and supernatant PRL content assays (N) in MMQ cells transfected with lentivirus expressing short hairpin RNA (Lv-shCD36) or scramble (Lv-NC). MOI = 75. SSO, sulfo-N-succinimidyl oleate.

$^{*}p < 0.05$, $^{**}p < 0.01$, and $^{***}p < 0.001$, n.s., not significant difference, vs. BSA group ($n = 3$ for independent experiments) or chow-fed mice ($n = 3$ for biological replicates). Student's t test and one-way ANOVA were used for statistical analysis.

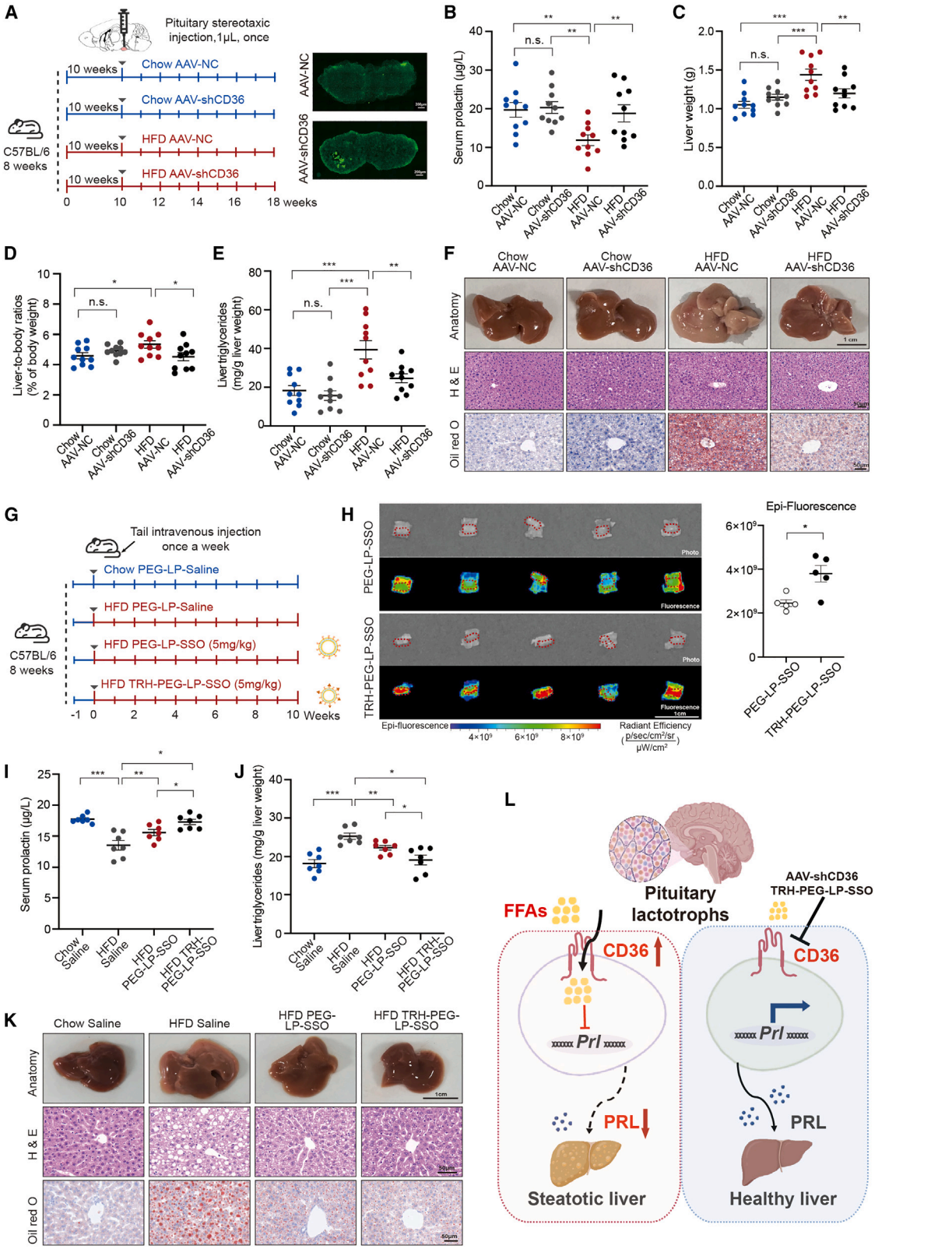

(legend on next page)

- Clinical measurements
- Fatty acids measurement by GC-MS
- Glucose tolerance test and insulin tolerance test
- Histological procedures
- Biochemical measurements
- RNA extraction and qRT-PCR assays
- Western blot analysis
- Immunofluorescent staining
- *In vitro* co-culture experiments
- Preparation of FFAs solutions
- Fatty acid uptake assays
- Cell viability assays
- Promoter luciferase reporter assay
- Intracellular calcium concentration measurement
- Inhibition of CD36 *in vitro*
- Preparation and characterization of TRH-PEG-LP-SSO and TRH-PEG-LP-DiR
- Evaluation of pituitary-targeted TRH-PEG-LP

● QUANTIFICATION AND STATISTICAL ANALYSIS

SUPPLEMENTAL INFORMATION

Supplemental information can be found online at https://doi.org/10.1016/j.celrep.2024.114465.

ACKNOWLEDGMENTS

We are grateful to all participants in our study. This work was supported by Natural Science Foundation of China grant awards (82030026, 81770819, 81900787, 82370841, and 81970704); the Natural Science Foundation of Jiangsu Province of China (BK20200118); the Six Talent Peaks Project of Jiangsu Province of China (YY-086); and Clinical Trials from the Affiliated Drum Tower Hospital, Medical School of Nanjing University (2021-LCYJ-PY-38 and 2021-LCYJ-DBZ-10). We also thank Charlesworth Author Services for professional English language editing.

AUTHOR CONTRIBUTIONS

Y.B. and P.Z. designed the experiments and supervised all aspects of the study. X.J. performed the experiments, analyzed the data, and wrote the manuscript. H.Y. conducted pituitary-targeted drug delivery system and analyzed the data. T.G. contributed to data collection and data analysis. H.X. and Y.N. performed the experiments. D.F., K.W., H.S., S.T., and T.W. contributed to clinic data collection. Y.B., P.Z., and X.J. wrote and edited the paper.

DECLARATION OF INTERESTS

The authors declare no competing interests.

Received: August 14, 2023
Revised: April 27, 2024
Accepted: June 24, 2024
Published: July 9, 2024

REFERENCES

1. Rinella, M.E., Lazarus, J.V., Ratziu, V., Francque, S.M., Sanyal, A.J., Kanwal, F., Romero, D., Abdelmalek, M.F., Anstee, Q.M., Arab, J.P., et al. (2023). A multisociety Delphi consensus statement on new fatty liver disease nomenclature. J. Hepatol. *79*, 1542–1556. https://doi.org/10.1016/j.jhep.2023.06.003.
2. Kanwal, F., Neuschwander-Tetri, B.A., Loomba, R., and Rinella, M.E. (2024). Metabolic dysfunction-associated steatotic liver disease: Update and impact of new nomenclature on the American Association for the Study of Liver Diseases practice guidance on nonalcoholic fatty liver disease. Hepatology *79*, 1212–1219. https://doi.org/10.1097/hep.0000000000000670.
3. Riazi, K., Azhari, H., Charette, J.H., Underwood, F.E., King, J.A., Afshar, E.E., Swain, M.G., Congly, S.E., Kaplan, G.G., and Shaheen, A.A. (2022). The prevalence and incidence of NAFLD worldwide: a systematic review and meta-analysis. Lancet. Gastroenterol. Hepatol. *7*, 851–861. https://doi.org/10.1016/s2468-1253(22)00165-0.
4. Younossi, Z., Anstee, Q.M., Marietti, M., Hardy, T., Henry, L., Eslam, M., George, J., and Bugianesi, E. (2018). Global burden of NAFLD and NASH: trends, predictions, risk factors and prevention. Nat. Rev. Gastroenterol. Hepatol. *15*, 11–20. https://doi.org/10.1038/nrgastro.2017.109.
5. Byrne, C.D., and Targher, G. (2015). NAFLD: a multisystem disease. J. Hepatol. *62*, S47–S64. https://doi.org/10.1016/j.jhep.2014.12.012.
6. Henderson, G.C. (2021). Plasma Free Fatty Acid Concentration as a Modifiable Risk Factor for Metabolic Disease. Nutrients *13*, 2590. https://doi.org/10.3390/nu13082590.
7. Kaikkonen, J.E., Jula, A., Viikari, J.S.A., Juonala, M., Hutri-Kähönen, N., Kähönen, M., Lehtimäki, T., and Raitakari, O.T. (2021). Associations of Serum Fatty Acid Proportions with Obesity, Insulin Resistance, Blood Pressure, and Fatty Liver: The Cardiovascular Risk in Young Finns Study. J. Nutr. *151*, 970–978. https://doi.org/10.1093/jn/nxaa409.
8. Jiang, L.P., and Sun, H.Z. (2022). Long-chain saturated fatty acids and its interaction with insulin resistance and the risk of nonalcoholic fatty liver disease in type 2 diabetes in Chinese. Front. Endocrinol. *13*, 1051807. https://doi.org/10.3389/fendo.2022.1051807.
9. Boden, G. (2006). Fatty acid-induced inflammation and insulin resistance in skeletal muscle and liver. Curr. Diabetes Rep. *6*, 177–181. https://doi.org/10.1007/s11892-006-0031-x.
10. Samuel, V.T., and Shulman, G.I. (2016). The pathogenesis of insulin resistance: integrating signaling pathways and substrate flux. J. Clin. Invest. *126*, 12–22. https://doi.org/10.1172/jci77812.

Figure 6. Inhibition of CD36 in the pituitary alleviated liver steatosis by improving PRL levels

(A) Experimental scheme of pituitary stereotactic adeno-associated virus (AAV)-injected mice (n = 10 per group). Scale bars, 200 μm.
(B) Quantification of serum levels of PRL of pituitary AAV-injected mice.
(C and D) Liver weights (C) and liver-to-body weight ratios (D) of pituitary AAV-injected mice.
(E and F) Liver TG content assays (E) and liver anatomy (scale bars, 1 cm), H&E staining (scale bars, 50 μm), and oil red O staining assays (scale bars, 50 μm) (F) of pituitary AAV-injected mice.
(G) Experimental scheme of pituitary-targeted drug delivery in mice (n = 7 per group). SSO, sulfo-N-succinimidyl oleate; TRH, thyrotropin-releasing hormone; PEG-LP, polyethylene glycol-modified liposomes.
(H) Fluorescence analysis of SSO delivery system localization in mice pituitary (n = 5 for biological replicates). Scale bars, 1 cm.
(I–K) Serum PRL content assays (I), liver TG content (J), and liver anatomy (scale bars, 1 cm), H&E staining (scale bars, 50 μm), and oil red O staining assays (scale bars, 50 μm) (K) of SSO-delivered mice.
(L) The proposed mechanism that the pituitary lactotrophs sensed excessive FFA signals and decreased PRL levels, thereby eliciting hepatic steatosis. Inhibiting excessive FFA uptake in pituitary through stereotactic injection or a specific drug delivery system effectively increased circulating PRL levels and ameliorated hepatic steatosis.
The data are presented as mean ± SEM. $^{*}p < 0.05$, $^{**}p < 0.01$, and $^{***}p < 0.001$, n.s., not significant difference. One-way ANOVA was used for statistical analysis.

11. Yan, F., Wang, Q., Lu, M., Chen, W., Song, Y., Jing, F., Guan, Y., Wang, L., Lin, Y., Bo, T., et al. (2014). Thyrotropin increases hepatic triglyceride content through upregulation of SREBP-1c activity. J. Hepatol. *61*, 1358–1364. https://doi.org/10.1016/j.jhep.2014.06.037.

12. Barb, C.R., Kraeling, R.R., and Rampacek, G.B. (1995). Glucose and free fatty acid modulation of growth hormone and luteinizing hormone secretion by cultured porcine pituitary cells. J. Anim. Sci. *73*, 1416–1423. https://doi.org/10.2527/1995.7351416x.

13. Zhang, P., Ge, Z., Wang, H., Feng, W., Sun, X., Chu, X., Jiang, C., Wang, Y., Zhu, D., and Bi, Y. (2018). Prolactin improves hepatic steatosis via CD36 pathway. J. Hepatol. *68*, 1247–1255. https://doi.org/10.1016/j.jhep.2018.01.035.

14. Hutchison, A.L., Tavaglione, F., Romeo, S., and Charlton, M. (2023). Endocrine aspects of metabolic dysfunction-associated steatotic liver disease (MASLD): Beyond insulin resistance. J. Hepatol. *79*, 1524–1541. https://doi.org/10.1016/j.jhep.2023.08.030.

15. Oh, J.Y., Osorio, R.C., Jung, J., Carrete, L., Choudhary, N., Lad, M., Saha, A., and Aghi, M.K. (2022). Transcriptomic Profiles of Normal Pituitary Cells and Pituitary Neuroendocrine Tumor Cells. Cancers *15*, 110. https://doi.org/10.3390/cancers15010110.

16. Fomina, A.F., and Levitan, E.S. (1995). Three phases of TRH-induced facilitation of exocytosis by single lactotrophs. J. Neurosci. *15*, 4982–4991. https://doi.org/10.1523/jneurosci.15-07-04982.1995.

17. Ben-Jonathan, N., and Hnasko, R. (2001). Dopamine as a prolactin (PRL) inhibitor. Endocr. Rev. *22*, 724–763. https://doi.org/10.1210/edrv.22.6.0451.

18. Grattan, D.R. (2015). 60 YEARS OF NEUROENDOCRINOLOGY: The hypothalamo-prolactin axis. J. Endocrinol. *226*, T101–T122. https://doi.org/10.1530/joe-15-0213.

19. Donnelly, K.L., Smith, C.I., Schwarzenberg, S.J., Jessurun, J., Boldt, M.D., and Parks, E.J. (2005). Sources of fatty acids stored in liver and secreted via lipoproteins in patients with nonalcoholic fatty liver disease. J. Clin. Invest. *115*, 1343–1351. https://doi.org/10.1172/jci23621.

20. Boden, G. (2011). Obesity, insulin resistance and free fatty acids. Curr. Opin. Endocrinol. Diabetes Obes. *18*, 139–143. https://doi.org/10.1097/MED.0b013e3283444b09.

21. Arab, J.P., Arrese, M., and Trauner, M. (2018). Recent Insights into the Pathogenesis of Nonalcoholic Fatty Liver Disease. Annu. Rev. Pathol. *13*, 321–350. https://doi.org/10.1146/annurev-pathol-020117-043617.

22. Zaidi, M., Yuen, T., and Kim, S.M. (2023). Pituitary crosstalk with bone, adipose tissue and brain. Nat. Rev. Endocrinol. *19*, 708–721. https://doi.org/10.1038/s41574-023-00894-5.

23. Guo, Z., Li, M., Han, B., and Qi, X. (2018). Association of non-alcoholic fatty liver disease with thyroid function: A systematic review and meta-analysis. Dig. Liver Dis. *50*, 1153–1162. https://doi.org/10.1016/j.dld.2018.08.012.

24. Møller, N., and Jørgensen, J.O.L. (2009). Effects of growth hormone on glucose, lipid, and protein metabolism in human subjects. Endocr. Rev. *30*, 152–177. https://doi.org/10.1210/er.2008-0027.

25. Li, J., Rice, M.S., Huang, T., Hankinson, S.E., Clevenger, C.V., Hu, F.B., and Tworoger, S.S. (2018). Circulating prolactin concentrations and risk of type 2 diabetes in US women. Diabetologia *61*, 2549–2560. https://doi.org/10.1007/s00125-018-4733-9.

26. Glintborg, D., Altinok, M., Mumm, H., Buch, K., Ravn, P., and Andersen, M. (2014). Prolactin is associated with metabolic risk and cortisol in 1007 women with polycystic ovary syndrome. Hum. Reprod. *29*, 1773–1779. https://doi.org/10.1093/humrep/deu133.

27. Xu, P., Zhu, Y., Ji, X., Ma, H., Zhang, P., and Bi, Y. (2022). Lower serum PRL is associated with the development of non-alcoholic fatty liver disease: a retrospective cohort study. BMC Gastroenterol. *22*, 523. https://doi.org/10.1186/s12876-022-02619-w.

28. Retnakaran, R., Ye, C., Kramer, C.K., Connelly, P.W., Hanley, A.J., Sermer, M., and Zinman, B. (2016). Maternal Serum Prolactin and Prediction of Postpartum β-Cell Function and Risk of Prediabetes/Diabetes. Diabetes Care *39*, 1250–1258. https://doi.org/10.2337/dc16-0043.

29. Shao, S., Yao, Z., Lu, J., Song, Y., He, Z., Yu, C., Zhou, X., Zhao, L., Zhao, J., and Gao, L. (2018). Ablation of prolactin receptor increases hepatic triglyceride accumulation. Biochem. Biophys. Res. Commun. *498*, 693–699. https://doi.org/10.1016/j.bbrc.2018.03.048.

30. Simcox, J., Geoghegan, G., Maschek, J.A., Bensard, C.L., Pasquali, M., Miao, R., Lee, S., Jiang, L., Huck, I., Kershaw, E.E., et al. (2017). Global Analysis of Plasma Lipids Identifies Liver-Derived Acylcarnitines as a Fuel Source for Brown Fat Thermogenesis. Cell Metabol. *26*, 509–522.e6. https://doi.org/10.1016/j.cmet.2017.08.006.

31. Fougerat, A., Schoiswohl, G., Polizzi, A., Régnier, M., Wagner, C., Smati, S., Fougeray, T., Lippi, Y., Lasserre, F., Raho, I., et al. (2022). ATGL-dependent white adipose tissue lipolysis controls hepatocyte PPARα activity. Cell Rep. *39*, 110910. https://doi.org/10.1016/j.celrep.2022.110910.

32. Freeman, M.E., Kanyicska, B., Lerant, A., and Nagy, G. (2000). Prolactin: structure, function, and regulation of secretion. Physiol. Rev. *80*, 1523–1631. https://doi.org/10.1152/physrev.2000.80.4.1523.

33. Han, J., Nepal, P., Odelade, A., Freely, F.D., Belton, D.M., Graves, J.L., Jr., and Maldonado-Devincci, A.M. (2020). High-Fat Diet-Induced Weight Gain, Behavioral Deficits, and Dopamine Changes in Young C57BL/6J Mice. Front. Nutr. *7*, 591161. https://doi.org/10.3389/fnut.2020.591161.

34. Park, Y.M. (2014). CD36, a scavenger receptor implicated in atherosclerosis. Exp. Mol. Med. *46*, e99. https://doi.org/10.1038/emm.2014.38.

35. Yang, X., Okamura, D.M., Lu, X., Chen, Y., Moorhead, J., Varghese, Z., and Ruan, X.Z. (2017). CD36 in chronic kidney disease: novel insights and therapeutic opportunities. Nat. Rev. Nephrol. *13*, 769–781. https://doi.org/10.1038/nrneph.2017.126.

36. Shu, H., Peng, Y., Hang, W., Nie, J., Zhou, N., and Wang, D.W. (2022). The role of CD36 in cardiovascular disease. Cardiovasc. Res. *118*, 115–129. https://doi.org/10.1093/cvr/cvaa319.

37. Zhao, L., Zhang, C., Luo, X., Wang, P., Zhou, W., Zhong, S., Xie, Y., Jiang, Y., Yang, P., Tang, R., et al. (2018). CD36 palmitoylation disrupts free fatty acid metabolism and promotes tissue inflammation in non-alcoholic steatohepatitis. J. Hepatol. *69*, 705–717. https://doi.org/10.1016/j.jhep.2018.04.006.

38. Zhao, Z., Ukidve, A., Kim, J., and Mitragotri, S. (2020). Targeting Strategies for Tissue-Specific Drug Delivery. Cell *181*, 151–167. https://doi.org/10.1016/j.cell.2020.02.001.

39. Kuda, O., Pietka, T.A., Demianova, Z., Kudova, E., Cvacka, J., Kopecky, J., and Abumrad, N.A. (2013). Sulfo-N-succinimidyl oleate (SSO) inhibits fatty acid uptake and signaling for intracellular calcium via binding CD36 lysine 164: SSO also inhibits oxidized low density lipoprotein uptake by macrophages. J. Biol. Chem. *288*, 15547–15555. https://doi.org/10.1074/jbc.M113.473298.

40. Zhao, G.K., Zheng, Y., Guo, H.X., Wang, H.Q., Ji, Z.H., Wang, T., Yu, S., Zhang, J.B., Yuan, B., and Ren, W.Z. (2022). TRH Regulates the Synthesis and Secretion of Prolactin in Rats with Adenohypophysis through the Differential Expression of miR-126a-5p. Int. J. Mol. Sci. *23*, 15914. https://doi.org/10.3390/ijms232415914.

41. Zhang, Q., Tang, J., Fu, L., Ran, R., Liu, Y., Yuan, M., and He, Q. (2013). A pH-responsive α-helical cell penetrating peptide-mediated liposomal delivery system. Biomaterials *34*, 7980–7993. https://doi.org/10.1016/j.biomaterials.2013.07.014.

42. He, Y., Zhang, L., and Song, C. (2010). Luteinizing hormone-releasing hormone receptor-mediated delivery of mitoxantrone using LHRH analogs modified with PEGylated liposomes. Int. J. Nanomed. *5*, 697–705. https://doi.org/10.2147/ijn.s12129.

43. Yang, C., Chen, F., Ren, P., Lofchy, L., Wan, C., Shen, J., Wang, G., Gaikwad, H., Ponder, J., Jordan, C.T., et al. (2020). Delivery of a model lipophilic membrane cargo to bone marrow via cell-derived microparticles. J. Contr. Release *326*, 324–334. https://doi.org/10.1016/j.jconrel.2020.07.019.

STAR★METHODS

KEY RESOURCES TABLE

REAGENT or RESOURCE	SOURCE	IDENTIFIER
Antibodies		
Prolactin antibody	Abcam	Cat# ab188229; RRID:AB_2921370
Pit-1 antibody	Abcam	Cat# ab273048
β-actin antibody	Proteintech	Cat# 60008-1-Ig; RRID:AB_2289225
CD36 antibody	Santa Cruz	Cat# sc-7309; RRID:AB_627044
TH antibody	Abcam	Cat# ab137869; RRID:AB_2801410
cFos antibody	Cell Signaling Technology	Cat# 2250; RRID:AB_2247211
Bacterial and virus strains		
pAAV2/9-U6-shCD36-CMV-EGFP-WPRE	Obio	N/A
pAAV2/9-U6-CMV-EGFP-WPRE	Obio	N/A
pRRLSIN-cPPT-U6-shRNA-SFFV-EGFP-SV40-puromycin	GeneChem	N/A
pRRLSIN-cPPT-U6-CON560-SFFV-EGFP-SV40-puromycin	GeneChem	N/A
Biological samples		
Blood samples from 24 MASLD subjects and 24 controls	This paper	N/A
Chemicals, peptides, and recombinant proteins		
C16-Bodipy	Thermo Fisher Scientific	Cat# D3821
Bodipy 493/503	Thermo Fisher Scientific	Cat# D3922
Sulfo-N-succinimidyl oleate	MedChemExpress	Cat# HY-112847
Thyrotropin-releasing hormone	MedChemExpress	Cat# HY-P1529
Palmitic acid	Sigma	Cat# P0500
Oleic acid	Sigma	Cat# O1008
Bovine serum albumin	Sigma	Cat# SRE0096
Critical commercial assays		
Mouse prolactin ELISA kit	FcMACS	Cat# FMS-ELM117
Mouse growth hormone ELISA kit	Cusabio	Cat# CSB-E07343m
Mouse thyroid-stimulating hormone ELISA kit	Cusabio	Cat# CSB-E05116m
Mouse follicle-stimulating hormone ELISA kit	Cusabio	Cat# CSB-E06871m
Mouse adrenocorticotropic hormone ELISA kit	Cusabio	Cat# CSB-E06874m
Mouse luteinizing hormone ELISA kit	Cusabio	Cat# CSB-E12770m
Mouse dopamine ELISA kit	Cusabio	Cat# CSB-E08661m
Rat prolactin ELISA kit	Raybiotech	Cat# ELR-PRL-1
Free fatty acids quantification kit	Sigma	Cat# MAK044
Dual Luciferase Reporter Assay Kit	Vazyme	Cat# DL101
Experimental models: Cell lines		
MMQ cells	Cell Culture Center of Xiehe Medical University (Beijing, China)	N/A
HepG2 cells	Cell Bank of the Shanghai Institute of Cell Biology (Chinese Academy of Sciences)	N/A
Experimental models: Organisms/strains		
Mouse: C57BL/6J	NBRI	Cat# N000013

(*Continued on next page*)

Continued

REAGENT or RESOURCE	SOURCE	IDENTIFIER
Oligonucleotides		
qRT-PCR primers	GenScript, in this paper (Table S8)	N/A
Software and algorithms		
SPSS	IBM	RRID: SCR_019096
Fiji-ImageJ	National Inst. Of Health	RRID: SCR_003070
GraphPad Prism	Graphpad	RRID: SCR_002798

RESOURCE AVAILABILITY

Lead contact

Further information and requests should be directed to and will be fulfilled by the lead contact, Yan Bi (biyan@nju.edu.cn).

Materials availability

This study did not generate new unique reagents.

Data and code availability

- All data reported in this paper will be shared by the lead contact upon request.
- This paper does not report original code.
- Any additional information required to reanalyze the data reported in this work paper is available from the lead contact upon request.

EXPERIMENTAL MODEL AND STUDY PARTICIPANT DETAILS

Human subjects

Eligible subjects aged between 18 and 70 years, who underwent liver biopsy to confirm hepatic steatosis and met the criteria for MASLD, were recruited from Nanjing Drum Tower Hospital between January 2018 and August 2022, including 64 control individuals and 264 MASLD subjects. Characteristics of the enrolled 328 subjects were summarized in Table 1. The cohort of individuals with normal glucose tolerance included 41 controls and 111 MASLD patients, and the characteristics of these subjects were shown in Table S2. Lipidomic profiles of serum FFAs in humans were identified by gas chromatography-mass spectrometry. This cohort consisted of 48 subjects, including 24 MASLD patients and 24 age- and sex-matched controls. The demographics and metabolic characteristics of these subjects were summarized in Table S7. Venous blood samples were collected after overnight fasting from each subject in a comparatively calm state to minimize the impact of external stimuli on PRL levels.

MASLD was diagnosed by having steatotic liver disease with any of a cardiometabolic risk factor (CMRF) in the absence of other causes of hepatic steatosis or excessive alcohol consumption ($\geq$140/210 g weekly, males/females). Cardiometabolic risk factors were defined as: a) body mass index (BMI) $\geq$ 25 kg/m^2 (23 kg/m^2 for Asia) or waist circumference (WC) $\geq$ 94 cm (males)/80 cm (females); b) fasting blood glucose (FBG) $\geq$ 5.6 mmol/L or 2-h post-load glucose $\geq$7.8 mmol/L or Hemoglobin A1c (HbA1c) $\geq$ 5.7% or type 2 diabetes or treatment for type 2 diabetes; c) blood pressure $\geq$130/85 mmHg or specific antihypertensive drug treatment; d) plasma triglycerides $\geq$1.7 mmol/L or lipid lowering treatment; e) plasma high-density lipoprotein-cholesterol (HDL-c) < 1.0 mmol/L (males) and <1.3 mmol/L (females) or lipid lowering treatment.[1] Liver steatosis score (S) was defined as the proportion of hepatocytes containing lipid droplets, with S0, S1, S2, and S3 indicating <5%, 5%–33%, 33%–66%, and >66%, respectively. Cases involving diseases or use of medications that may influence PRL levels (pituitary adenoma, corticosteroids, and antipsychotic drugs), viral hepatitis, hyperthyroidism or hypothyroidism, pregnancy, and type 1 diabetes were excluded.

Ethical approval of the study was granted by the Nanjing Drum Tower Hospital Ethics Committee (Approval Numbers: 201701701 and 201703008). All patients and control individuals meeting the inclusion criteria gave consent at the time of enrollment. The study adhered to the declaration of Helsinki guidelines.

Animal models

All experimental animals were handled humanely. Animal experiment protocols were approved by the Institutional Animal Care Guidelines of Nanjing University. Healthy 6- to 8-week-old female C57BL/6J mice were fed a high-fat diet (HFD) containing 60% fat (Research Diets, USA) for 10 weeks. As controls, age-matched mice were fed a standard normal diet (chow). Bilateral stereotaxic injections were conducted by injecting the pituitary gland with DMSO (vehicle) at 500 nL/side or with 5 mM or 10 mM C16-Bodipy, a fluorescently labeled palmitic acid, at 500 nL/side (Invitrogen) for 24, 48, or 72 h. To inhibit CD36 expression in the pituitary, 1 μL of adeno-associated viruses (AAV-ShCD36, 1.2 × 10^9 viral genomes (vg); sequence: GCCATAATTGAGTCCTATAAA; OBiO, China) or control (AAV-NC; 1.6 × 10^9 vg; sequence: CCTAAGGTTAAGTCGCCCTCG; OBiO, China) was bilaterally injected into the pituitary

glands of HFD-fed mice. The stereotaxic coordinates of pituitary relative to the bregma were as follows: anteroposterior: −2.5 mm, mediolateral: ±0.15 to 0.25 mm, and dorsoventral: −6.35 to 6.45 mm. All mice were sacrificed after overnight fasting.

Polyethylene glycol-modified liposomes loaded with sulfo-N-succinimidyl oleate (SSO, CD36 antagonist) were prepared via lipid film hydration and ultrasonic dispersion (PEG-LP-SSO). TRH-PEG-DSPE was conducted by combining thiolated thyrotropin-releasing hormone (TRH) with Mal-PEG2000-DSPE and then incubated with PEG-LP-SSO to obtain TRH-PEG-LP-SSO. The particle size distribution and zeta potential of prepared drug loaded liposomes and blank liposomes were determined by laser particle size analyzer (Brookhaven, USA). Pituitary targeting by TRH-PEG-LP-SSO was assessed using small animal imaging instruments. PEG-LP-Saline (as control), PEG-LP-SSO (5 mg/kg) and TRH-PEG-LP-SSO (5 mg/kg) were administered once weekly to 8-week-old mice through tail vein injection. The mice were maintained on the HFD or chow diet for 10 weeks. Blood and liver samples were collected for further analysis at indicated time points.

Cell experiments

MMQ cells, deriving from rat prolactinoma that exclusively secrete PRL and behave like normal lactotrophs, were obtained from the Cell Culture Center of Xiehe Medical University (Beijing, China). The MMQ cells were fasted in Ham's F12 medium for 2 h and then incubated with 10% fatty acid-free bovine serum albumin (BSA) or mixtures of palmitic acid and oleic acid (PAOA) at a 1:1 ratio, each at concentrations of 25, 50, 75 and 100 μM (Sigma) for 24 h.

METHOD DETAILS

Clinical measurements

Individuals without previously diagnosed type 2 diabetes mellitus (T2DM) were subjected to a 75 g oral glucose tolerance test (OGTT) after an overnight fast of at least 8 h. Impaired glucose regulation (IGR): 5.6 mmol/L $\leq$ fasting blood glucose (FBG) < 7.0 mmol/L and 2 h blood glucose (BG) < 7.8 mmol/L; or FBG <5.6 mmol/L and 7.8 mmol/L $\leq$ 2 h BG < 11.1 mmol/L. T2DM was defined as patients having at least one of the following: history or current use of antidiabetic medication, or FBG $\geq$7.0 mmol/L or 2 h BG $\geq$ 11.1 mmol/L, or HbA1c $\geq$ 6.5%. FBG was measured using a hexokinase method (TBA-200FR, Japan). Fasting insulin (FINS) was determined by an electro chemiluminescent immunoassay (Roche, USA). Homeostasis model assessment of insulin resistance (HOMA-IR) was calculated by FBG (mmol/L) × FINS (uIU/L)/22.5. HbA1c was measured by HPLC (HLC-73G8, Japan). Free fatty acids (FFAs) were measured by enzymatic methods (DiaSys Diagnostic Systems, Germany). Serum aspartate aminotransferase (AST), alanine aminotransferase (ALT), total cholesterol (TC), triglyceride (TG), low-density lipoprotein (LDL) cholesterol and HDL-c were detected using an autoanalyzer (Abbott Laboratories, USA). Serum prolactin (PRL), adrenocorticotropic hormone (ACTH), thyrotropin-stimulating hormone (TSH), luteinizing hormone (LH), follicle-stimulating hormone (FSH) and growth hormone (GH) were detected using an automated chemiluminescent immunoassay (Siemens Immulite 2000, Germany).

Fatty acids measurement by GC-MS

A targeted metabolic analysis approach using gas chromatography-mass spectrometry (GC-MS) determinates 35 medium and long-chain fatty acids in the serum of human and mice. The derivatized samples were analyzed by a Thermo GC-MS system (Thermo Scientific, USA). The capillary column Thermo TG-FAME (50 m × 0.25 mm ID × 0.20 μm) was used to separate and determine metabolites. The injection volume was 1.0 μL. The temperatures of the injection and the ion source were adjusted to 250°C and 300°C, respectively. The initial oven temperature was set at 80°C for 1 min, and then increased with a rate of 20°C per minute to 160°C for 1.5 min, then raised with a rate of 3°C per minute to 196°C for 8.5 min, and then raised with a rate of 20°C per minute to 250°C for 3 min. The carrier gas was high-purity helium and the flow rate was set to 0.63 mL/min. Electron ionization voltage was set as 70 eV. The concentrations of target fatty acids were calculated by dividing the analyte peak are of the target metabolite by that of the respective internal standard and then multiplying by the slope of the external calibration curve.

Glucose tolerance test and insulin tolerance test

For glucose tolerance tests (GTT), fasting blood glucose levels were measured after a 16-h fast. Mice were intraperitoneal injected with glucose (2 g/kg body weight). Blood glucose levels were recorded after 15-, 30-, 60-, 90- and 120-min using blood obtained via tail vein. For insulin tolerance tests (ITT), mice were fasted for 4 h and the intraperitoneal injected with insulin (0.5 units/kg body weight). Blood glucose levels were recorded after 15-, 30-, 60-, 90- and 120-min using blood from tail vein.

Histological procedures

For Hematoxylin & Eosin staining (H&E staining), fresh liver samples were fixed in 4% paraformaldehyde (PFA) for at least 24 h, and then dehydrated by using 70%, 80% and 90% alcohol and embedded in paraffin. 4 μm sections were stained with a standard Hematoxylin and Eosin alcoholic procedure according to the manufacturer's instructions (GP1031, Servicebio, Wuhan).

For Oil red O staining, frozen liver samples were cut in sections of 8 μm with a cryostat (CM1950, Leica Biosystems, Germany) and stained in filtered Oil red O working solution for 10 min. After being washed in distilled water, sections were counterstained with Mayer's hematoxylin for 5 min and mounted in aqueous mounting (glycerin jelly). A similar procedure of Oil red O staining was performed for MMQ cells.

Lipid drops ultrastructure in mice hepatocytes were evaluated by transmission electron microscopy (TEM). Mice liver was dissected and fixed in 2.5% glutaraldehyde for 2 h and 1% osmium tetroxide for 1 h at 4°C, then dehydrated and embedded in epoxy resin. Liver tissue was sliced by an ultramicrotome (RMC/MTX, Elexience). Ultrathin sections (60–80 nm thickness) were observed with transmission electron microscope (HT7800, HITACHI, Beijing).

Biochemical measurements

The levels of free fatty acids (Sigma, USA), prolactin (FcMACS, China; Raybiotech, USA) were measured using enzyme linked immunosorbent assay (ELISA) kits according to the manufacturers' instructions. Serum GH, TSH, ACTH, FSH and LH levels, dopamine levels in hypothalamic arcuate nucleus were measured using mice ELISA kits (Cusabio, China). Serum ALT, AST, TG, TC levels were determined using an automatic biochemical analyzer (Chemray 800, Rayto, China).

RNA extraction and qRT-PCR assays

The mRNA levels were determined using quantitative real-time PCR (qRT-PCR). Briefly, total RNA was extracted using Trizol (Invitrogen, USA). Reverse transcription was done using a Prime Script RT reagent kit (Takara, Japan). qRT-PCR was done using an SYBR RT-PCR mix on a Light Cycler 480 system (Roche, Switzerland).

Western blot analysis

For western blot analyses, protein was extracted from tissues and cells by RIPA lysis buffer and quantified by BCA protein assay kit (Thermo Scientific, USA). Forty micrograms of protein lysates were loaded into 10% SDS-PAGE gels and then transferred onto polyvinylidene difluoride (PVDF) membranes (Millipore, USA). The membranes were incubated with primary antibodies, followed by incubation with secondary antibodies.

Immunofluorescent staining

Mice brains were collected after intracardially perfusion with phosphate-buffered saline (PBS) and 4% paraformaldehyde (PFA) sequentially, and then were fixed in 4% PFA for 24 h, followed by soaking in 15% and 30% sucrose solution for dehydration. Brains were sliced into 20 μm coronal sections using a freezing microtome (Leica CM 1950) and incubated overnight with antibody to tyrosine hydroxylase (TH) (1:100, Abcam) and cFos (1:1000, CST), followed by incubation with appropriate fluorescent secondary antibodies for 1 h at room temperature. Slices were stained with DAPI before photographed using a Leica TCS SP8-MaiTai MP confocal microscope, followed by blind intensity analysis using ImageJ software.

In vitro co-culture experiments

For co-culture experiment, MMQ cells were cultured in a *trans*-well system placed above the HepG2 cells at different cell counts, ranging from 30-, 60- and 90 × 10^4 cells. The HepG2 cells were incubated with 250 μM PAOA or equal volume of BSA for 24 h and then Oil red O staining and triglyceride quantification assays were performed.

Preparation of FFAs solutions

50 mmol/L (mM) palmitic acid (PA) solution was prepared by adding 0.128 g PA to 10 mL of 0.1 mol/L NAOH solution and placed in a water bath at 75°C for 30 min. It was then added to 10% fatty acid-free bovine serum albumin (BSA) solution and diluted to 5 mM working solution. 50 mM oleic acid (OA) solution was prepared by adding 0.141 g OA to 10 mL of 0.1 mol/L NAOH solution and then diluted to 5 mM working solution by 10% BSA solution.

Fatty acid uptake assays

The fatty acid uptake assay was done by incubating MMQ cells with 1 μM C16-Bodipy (Invitrogen, USA) for 30 min at indicated concentrations followed by uptake assessment using flow cytometry.

Cell viability assays

Cell viability was detected by Cell Counting Kit 8 (CCK-8, Vazyme, China) assay kit according to the manufacturer's instructions. MMQ cells were seeded into a 96-well plate at 20,000 cells per well with 90 μL Ham's F12 without fetal bovine serum and fasted for 2 h. After starvation, cells were treated with various concentrations of FFAs for 24 h. 10 μL CCK-8 solution was then added into each well and incubated in the dark for 2 h at 37°C. Absorbance was detected at 450 nm wavelength by Vector 5 (Bio-Tech Instruments, USA).

Promoter luciferase reporter assay

A rat *Prl* fragment flanking −2000 bp to 0 bp was cloned into the pGL3-basic vector. The MMQ cells were pre-treated with 25 μM SSO or equal volume of DMSO for 24 h before PAOA exposure. After incubated with PAOA for additional 24 h, the cells were co-transfected with promoter constructs and Pit-1 expression plasmids (GenePharma, China) for another 48 h. The luciferase activity was measured with the dual-luciferase reporter assay kit (Promega). Renilla luciferase activity was used as an internal control.

Intracellular calcium concentration measurement

The intracellular Ca^{2+} concentration of MMQ cells was measured using FLIPRTetra system (Molecular Devices, Sunnyvale, CA, USA). After 2-h fast, MMQ cells were incubation with the calcium indicator Fluo-4/AM (4 μM) for 1 h and were then gently rinsed with pre-warmed Locke's buffer (in mM: HEPES 8.6, KCl 5.6, NaCl 154, D-glucose 5.6, MgCl2 1.0, $CaCl_2$ 2.3 and glycine 0.1, pH 7.4) four times with a final volume of 150 μL per well. The plate was then loaded onto the imaging chamber of fluorescent imaging plate reader (FLIPRTetra system, Molecular Devices). After an equilibration period of 2 min, mobilization of intracellular calcium was recorded for 5 min followed by the addition of vehicle (10% bovine serum albumin) or different concentrations of free fatty acids working solution (25 μL, 7× final concentration) by an automated and programmable pipetting system. The fluorescent signals (F) were detected at a sampling rate of 1 Hz. Data were presented as F/F0, where F0 was the minimal arbitrary fluorescence unit before treatment. The curves of F/F0 were plotted by Prism GraphPad software (version 9). One-way analysis of variance (ANOVA) followed by post hoc Bonferroni comparison were used to compare the statistical significance among different groups.

Inhibition of CD36 *in vitro*

To inhibit CD36, MMQ cells were pre-treated with SSO, at 10, 25, 50 μM, respectively, for 24 h or transfected with 3×10^9 TU/mL of lentivirus expressing short hairpin RNA (Lv-shCD36; sequence: CACAGATTTGTTCTTCCAGCCAA; GeneChem, China) for 72 h before exposure to PAOA. SSO vehicle or 3×10^9 TU/mL of Lv-NC (sequence: TTCTCCGAACGTGTCACGT; GeneChem, China) were used as controls. PRL levels were determined using mouse (Fc MACS, China) and rat (Raybiotech, USA) prolactin ELISA kits. Oil red O staining and triglyceride kits (Applygen, China) were used to determine the TG content in MMQ cells.

Preparation and characterization of TRH-PEG-LP-SSO and TRH-PEG-LP-DiR

TRH-PEG-LP-SSO was prepared by the thin-film hydration method as described.[41] To prepare liposomes (PEG-LP), HSPC, cholesterol, and mPEG2000-DSPE (molar ratio = 62.5:37.5:0.4) were dissolved in chloroform.[42] SSO-loaded liposomes were prepared by adding SSO to the lipid organic solution before the solvent evaporation. Likewise, an appropriate amount of DiR was added to the solution before the solvent evaporation to prepare DiR-loaded in liposomes. Then the organic solvent was removed by rotary evaporation, and the film was hydrated in physiological saline. The mixture was ultrasonicated for 3 min to obtain Lip/SSO or Lip/DiR. TRH reacted with Traut's reagent to obtain thiolated TRH, which reacted with Mal-PEG2000-DSPE to obtain TRH-PEG-DSPE. Then the TRH-PEG-DSPE solution was added to the preformed Lip/SSO or Lip/DiR solution at TRH-PEG-DSPE: phospholipid molar ratios (1:1000) and incubated at 60°C for 1 h to obtain TRH-PEG-LP-SSO or TRH-PEG-LP-DiR. The particle size distribution and zeta potential of prepared drug loaded liposomes and blank liposomes were determined by laser particle size analyzer (Brookhaven, USA). The concentration of SSO was determined by measuring the fluorescence intensity of Bodipy labeled SSO. The excitation and emission wavelengths are 493nm and 503nm, respectively (SpectraMax iD3, USA). The unencapsulated SSO was collected through ultrafiltration centrifuge tubes (3000 Da, Millipore, Billerica, MA) to calculate the encapsulation efficiency of SSO. All results were the mean of three tests, and all data are shown as mean ± standard deviation (SD).

Evaluation of pituitary-targeted TRH-PEG-LP

TRH-PEG-LP-DiR or PEG-LP-DiR was injected into mice tail vein for 2 h, where the final concentration of DiR in the delivery system is 15 μg/mL. Using the small animal live imaging device, the fluorescence intensity of dissected pituitary tissue was observed at an excitation wavelength of 750 nm and an emission wavelength of 780 nm, to evaluate the pituitary-targeted TRH-PEG-LP.[43]

QUANTIFICATION AND STATISTICAL ANALYSIS

Data analyses were done on SPSS Version 26.0 (IBM Inc., USA). Continuous variables were presented as mean ± standard deviation or median with interquartile range (IQR). Categorical variables were presented as counts (%). The Mann–Whitney U test and Kruskal-Wallis analysis were used to compare two groups or multiple groups, respectively. Logistic regression models were used to estimate odds ratios (OR) with 95% confidence intervals (95% CI). Mediation analyses were performed using the PROCESS to example the mediating effect of decreased PRL levels involved in the association between FFAs and MASLD. For cell experiments, data were summarized as mean ± SEM. Statistical comparisons were made using unpaired t test or one-way ANOVA on GraphPad Prism, version 9.0. $p < 0.05$ indicates statistically significant differences.